

Ground state entanglement in quantum spin chains

J. I. Latorre,¹ E. Rico,¹ and G. Vidal²

¹Dept. d'Estructura i Constituents de la Matèria, Univ. Barcelona, 08028, Barcelona, Spain.

²Institute for Quantum Information, California Institute for Technology, Pasadena, CA 91125 USA

(Dated: 9th February 2020)

A microscopic calculation of ground state entanglement for the XY and Heisenberg models shows the emergence of universal scaling behavior at quantum phase transitions. Entanglement is thus controlled by conformal symmetry. Away from the critical point, entanglement gets saturated by a mass scale. Results borrowed from conformal field theory imply irreversibility of entanglement loss along renormalization group trajectories. Entanglement does not saturate in higher dimensions which appears to limit the success of the density matrix renormalization group technique. A possible connection between majorization and renormalization group irreversibility emerges from our numerical analysis.

PACS numbers: 03.67.-a, 03.65.Ud, 03.67.Hk

I. INTRODUCTION

At zero temperature, correlations in a quantum many-body system are not due to statistical fluctuations but to the intricate structure of its ground state. The degree of complexity of this structure may vary, ranging from the trivial case —e.g. when an external magnetic field aligns in its direction all the spins of a lattice, producing a product or unentangled state—, to situations where the specific form of the ground state is so entangled that can not even be computed, as it is the case for most interacting systems. Thus, quantum entanglement naturally appears in low temperature many-body physics. It accounts for many of its important aspects, such as the long-range correlations that characterize a quantum phase transition but, at the same time, its complicated structure very often poses an insuperable obstacle to numerical studies.

There are a number of good reasons to study entanglement in quantum many-body systems. On the one hand, over the last decade entanglement has been realized to be a crucial resource to process and send information in novel ways [1]. It is, for instance, the key ingredient in quantum information tasks such as quantum teleportation and superdense coding, and it also appears in most proposed algorithms for quantum computation [2]. This has triggered substantial experimental efforts to produce entanglement in engineered quantum systems [3]. Consequently, it makes a lot of sense to explore those systems in which entanglement is present in a natural way, with a view either to extract it to process quantum information or else to gain insight into physical mechanisms that can be used to entangle a large number of quantum systems.

But the motivation of such studies need not refer to the potential applications of entanglement as a resource in quantum information processing. The ground state of a typical quantum many-body system consists of a superposition of a huge number of product states. Understanding this structure is equivalent to establishing how and to what extent subsystems are interrelated, which in turn is what determines many of the relevant properties

of the system. In this sense, the study of multipartite entanglement offers an attractive theoretical framework from which one may be able to go beyond customary approaches to quantum collective phenomena [4], and thereby gain new insights into relevant quantum effects such as superconductivity [5], quantum Hall effect [6] and quantum phase transitions [7]. Most promisingly, a theory of entanglement in many-body systems may also lead to the development of new numerical techniques. In particular, recent results suggest that through a suitable parameterization of quantum superpositions it is indeed possible to efficiently simulate a large class of quantum systems [8].

In this paper we present a quantitative analysis of entanglement in several one-dimensional spin models, expanding and completing the results of Ref. [9]. The models we discuss fulfill a convenient combination of requirements: they are solvable —the ground state can be computed by using a number of well-known analytical and numerical techniques— and at the same time they successfully describe a rich spectrum of physical phenomena, which include ordered and disordered magnetic phases connected by a quantum phase transition [7].

The paper has been divided into five more sections. A brief summary of them follows.

The study of entanglement in a system with many particles can be approached in several complementary ways [9, 10, 11, 12, 13, 14, 15, 16, 17] and we shall start by explaining in section II on which specific aspects of a spin-chain ground state we focus here. Our aim will be to determine the degree of entanglement between a *block* of spins and the rest of the chain, as measured by the von Neumann entropy of the block, and to investigate how it grows with the size of the block. Perhaps the best way to justify such a particular choice is by referring to the rich spectrum of conclusions that can be drawn from the results we have obtained.

Sections III and IV are devoted, respectively, to computing the entropy of a spin block for the XY model and for the XXZ model. The calculation is divided into two parts. First, we construct the ground state of the spin

chain, which for general chains is a highly non-trivial problem. Fortunately, the XY model can be treated analytically even in the limit of an infinite chain. Similarly, for the XXZ model well-known techniques can be used to easily cope with chains consisting of up to twenty spins. Then, from the ground state of each model we extract the entropy of a spin block. For the XY model this is shown to build down to diagonalizing a matrix whose dimensions grow only quadratically with the size of the block. In this way we compute the entanglement for blocks of up to several hundreds of spins. In the XXZ, instead, we only consider blocks of up to ten qubits, but the results can already be convincingly interpreted as an independent confirmation of the conclusions drawn from the XY model.

In section V we discuss the findings of the previous two sections. Away from a critical point, in both the XY and XXZ models the entropy of a block of spins, a function that turns out to grow monotonically with the number of spins, achieves a finite *saturation* value for block sizes larger than the correlation length of the system. Instead, the same quantity grows unboundedly at a quantum phase transition, where the correlation length diverges. More specifically, the entropy for a critical chain grows logarithmically in the size of the spin block, with a multiplicative coefficient that depends only on the universality class of the phase transition. That is, at the critical point entanglement obeys universal scaling laws.

Interestingly, the behavior of the entanglement in a critical spin chain matches well-known results in conformal field theory, where the geometric entropy –analogous to the spin-block entropy, but defined in the continuum– has been computed for 1+1 dimensional theories [18, 19, 20, 21]. The geometric entropy grows logarithmically with the size of the interval under consideration and with a multiplicative constant given by the *central charge* of the theory. As described in section VI, a consistent picture arises. At a critical point the large-scale behavior of a spin chain is universal, with the QPT belonging to a given universality class. All long-range properties of the chain are then described by the conformal field theory associated to that universality class, and in particular the entanglement between a block of spins and the rest of the chain follows the same law as the geometric entropy.

The above connection between entanglement and the geometric entropy of conformal theories has several implications. Previous calculations of the entropy in higher dimensions indicate that in 2 and 3 dimensional spin lattices the entropy of a spin block grows as the size of the surface of the block —the same law holding both for critical and non-critical lattices. This lack of saturation of the entropy seems to be responsible for undermining the performance of the DMRG technique [22]. Thus, we interpret in terms of entanglement why this technique —so successful for non-critical spin chains— deteriorates in critical one-dimensional lattices and fails to work properly both for critical and non-critical chains and in two- and three-dimensional lattices [23].

The scaling law obeyed by the entropy can also be understood as an increase of disorder in the vacuum when the size of the spin block grows. The measure of ordering provided by the entropy can be further refined and shown to emerge from majorization relations between the vacuum density matrices.

Finally, we translate the results related to the c-Theorem [24] to quantum information. Entanglement is argued to decrease along renormalization group trajectories. A number of numerical and analytical results are consistent with the idea that irreversibility of renormalization group flows may be rooted on a majorization ordering of the vacuum density matrices along the flow.

II. ENTANGLEMENT MEASURES IN A QUANTUM SPIN CHAIN

A major difficulty in studying the entanglement in a many-body quantum system comes from the fact that the number of degrees of freedom grows exponentially with the number of interacting subsystems. In particular, the task of computing explicitly the ground state of a large number of spins in a chain, to then analyze its entanglement properties, turns out to be very difficult, if not unsurmountable.

Fortunately, for some specific spin models the ground state has been previously computed. One can then try to characterize entanglement in these models. This is once again a rather ambitious enterprise. On the one hand, it entails serious computational difficulties, since the corresponding ground states, when expressed in a local basis, still involve exponentially many coefficients. On the other hand such characterization is also challenging from a conceptual viewpoint. The study of entanglement of a large number of particles is a relatively unexplored subject and it has not yet even been established what aspects of a ground state a sensible characterization should consider. Therefore, an important part of the problem is to actually identify which quantities may be of interest.

This section is devoted to describe and motivate our particular approach, which attempts to characterize the ground state of the spin chain through the spectral properties of the reduced density matrix for a block of spins. We start by reviewing previous work.

A. Quantifying N-partite entanglement

A state $|\Psi\rangle \in \mathcal{H}_2^{\otimes N}$ of N spins is entangled if it cannot be written as the tensor product of single-spin states,

$$|\Psi\rangle \neq |\psi_1\rangle \otimes |\psi_2\rangle \otimes \cdots \otimes |\psi_N\rangle. \quad (2.1)$$

Product states depend on $\mathcal{O}(N)$ parameters and are therefore just a subset of zero measure in the set of states of N spins. An entangled state can always be expressed as a linear combination of $\mathcal{O}(2^N)$ product states (say, by expanding $|\Psi\rangle$ in a product basis). Characterizing

entanglement is about simplifying the set of entangled states, for instance by uncovering structures and identifying those parameters that are particularly relevant from a physical or computational point of view.

In recent years a quantitative theory of bipartite entanglement has been developed based on the possibility of converting one entangled state $|\Psi\rangle$ into another entangled state $|\Psi'\rangle$ by applying local operations on each of the subsystems [25]. The basic idea is that if the state $|\Psi\rangle$ can be converted into the state $|\Psi'\rangle$, then the former cannot be less entangled than the latter [or else one could increase quantum correlations through local manipulation, but this can at most introduce classical correlations between the subsystems]. Thus, local convertibility allows us to *compare* the entanglement of different states.

Two simple characterizations are then possible for systems with $N = 2$ subsystems with local Hilbert spaces of arbitrarily large dimension. (i) In an asymptotic sense, any entangled state $|\Psi\rangle_{AB}$ of spins A and B is equivalent (*i.e.*, reversible convertible) to some fraction $E(\Psi)$ of an EPR state,

$$\frac{1}{\sqrt{2}}(|0\rangle_A \otimes |0\rangle_B + |1\rangle_A \otimes |1\rangle_B). \quad (2.2)$$

Here the *entropy of entanglement* $E(\Psi)$ [26] corresponds to the von Neumann entropy of the reduced density matrix $\rho_A \equiv \text{tr}_B |\Psi\rangle\langle\Psi|$ for one of the spins,

$$E(\Psi) \equiv -\text{tr}(\rho_A \log_2 \rho_A). \quad (2.3)$$

(ii) The convertibility of a single copy of $|\Psi\rangle$ by local operations depends exclusively on the spectrum of ρ_A through a finite set of *entanglement monotones* [27] (entanglement measures for the non-asymptotic case). Deterministic local conversions of state $|\Psi\rangle$ into state $|\Psi'\rangle$ [28] are ruled by the majorization relation, to be introduced later in Eq. (2.16).

None of these results have been successfully generalized to $N > 2$ subsystems. Already for $N = 3$ subsystems, asymptotic conversions appear to no longer be reversible [29], while single-copy conversions are hardly possible [30]. The situation is even worse for increasing N . The number of coefficients characterizing $|\Psi\rangle$ grows exponentially in N , while the increase in parameters that can be controlled locally is only linear. As a result, for instance, two states $|\Psi\rangle$ and $|\Psi'\rangle$ are often not connected by local operations, not even in the most allowing scenario, where conversions are required to succeed with just some finite probability. More specifically, for $N = 3$ qubits there are two inequivalent classes of states under stochastic local operations, while for $N > 3$ qubits an infinite number of such classes exist, rendering the approach impractical [31] (see ref. [32] for an exhaustive enumeration of the infinitely many classes for $N = 4$ qubits).

Thus, in spite of the remarkable success achieved in the bipartite case, local manipulations are not such good a guidance to comprehensively characterize multipartite entanglement. Other possibilities should be considered

instead. For instance, one could base the characterization on the complexity of preparing a quantum state (or a series of quantum states involving an increasing number of particles) by only two-particle unitary operations. Parameter counting shows that one can distinguish, for instance, between (families of) states requiring polynomially many such operations and those requiring exponentially many operations. Alternatively, one can study the computational cost of classically simulating the evolution of the quantum many-body system when initially prepared in a given state [33]. Also, one can consider how entanglement is affected by a change of scale in the system. In any case, further study in this direction is certainly still required.

Nevertheless, it is still both possible and useful to analyze bipartite properties of a state of many spins. For instance, one may study the entanglement between every two spins in a chain. In this case, entanglement can be measured using the *concurrence*, which is defined for the reduced density matrix of a pair of spins [34] when tracing out the rest of the chain. The choice of the pair can be made so as to scan the system in order to infer how bipartite entanglement is distributed.

Along these lines, in ref. [11] the nearest neighbor concurrence was expressed as a function of the energy of the pair of spins and found not to be maximized by the ground state of an antiferromagnetic spin chain. Similarly, concurrence was also analyzed in ref. [12, 13] in the Ising and the Heisenberg chain, obtaining that there are some values of the temperature and the external uniform magnetic field for which the concurrence at nearest neighbors is greater than the one at zero temperature or zero magnetic field.

Later, it was pointed out in ref. [15, 16] that, at zero temperature and for the Ising model with magnetic field, the concurrence at nearest neighbors has a maximum near the critical magnetic field, and that for next to nearest neighbor the maximum is just at the critical point. This fact was interpreted in terms of the property of monogamy of the concurrence, previously introduced in ref. [10]. A notable fact is that the concurrence seems to disappear at third nearest neighbors. In practice, this can be understood as a shortcoming for using a two-qubit measure in order to capture the global distribution of entanglement along the chain.

B. Entropy of a block of spins

The approach we propose here is also based on bipartite entanglement. We consider a block of adjacent spins and study its entanglement with the rest of the spin chain. We are particularly interested in how the entanglement between the block and the chain depends on the size of the block. In this way, we expect to be able to explore the behavior of quantum correlations at different length scales, not by looking at two increasingly separated subsystems (as in the above studies involving

the concurrence), but by progressively increasing the size of one of them. Later on in this section we will provide a more pragmatic justification for our choice, in terms of numerical schemes for the simulation of spin chains.

Let $|\Psi_g\rangle$ denote the ground state of a chain of N spins and let ρ_L ,

$$\rho_L \equiv \text{tr}_{N-L} |\Psi_g\rangle\langle\Psi_g|, \quad (2.4)$$

be the reduced density matrix for L contiguous spins. In the models we shall discuss, the ground state $|\Psi_g\rangle$ is translationally invariant, so that ρ_L does not depend on the position of the block of spins but only on its size L . Because the chain is in a pure state, all the information about the entanglement between the block of spins and the rest of the chain is contained in the eigenvalues of ρ_L . If ρ_L is a pure state itself, then the block is unentangled from the chain. Instead, if ρ_L has many non-zero eigenvalues, this roughly indicates a lot of entanglement between the block and the chain. As a matter of fact, the whole spectrum of ρ_L is of interest, as we shall discuss shortly. For concreteness, however, we will mainly use as a measure of entanglement a single function of the spectrum of ρ_L , the von Neumann entropy S_L ,

$$S_L \equiv -\text{tr}(\rho_L \log_2 \rho_L). \quad (2.5)$$

This choice corresponds to the *entropy of entanglement* [26] between the block and the rest of the chain (recall Eq. (2.3)).

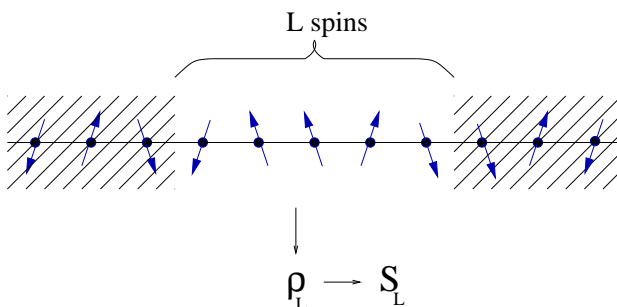


Figure 1: S_L corresponds to the entropy of the reduced density matrix ρ_L for a block of L adjacent spins. ρ_L is obtained from the ground state $|\Psi_g\rangle$ of the N spins that constitute the chain by tracing out all spins outside the block.

1. Properties of the entropy of a block of spins

Let us discuss some general properties of S_L as a function of L . By construction, we have that S_L is positive,

$$S_L \geq 0, \quad L = 0, 1, \dots, N, \quad (2.6)$$

where we have defined $S_0 \equiv 0$. Because the chain is in a pure state, the spectrum of the reduced density matrix

for a block of spins and for the rest of the chain are the same. In particular, the two parts will also have the same entropy. Recalling that the ground state is translationally invariant, we have

$$S_L = S_{N-L}, \quad L = 0, 1, \dots, N. \quad (2.7)$$

In addition, S_L is a concave function,

$$S_L \geq \frac{S_{L-M} + S_{L+M}}{2}, \quad (2.8)$$

where $L = 0, \dots, N$, and $M = 0, \dots, \max\{N-L, L\}$. This can be proved with the help of the strong subadditivity of the von Neumann entropy [2, 35],

$$S(ABC) + S(B) \leq S(AB) + S(BC), \quad (2.9)$$

where A , B and C are three subsystems and, say, $S(AB)$ denotes the entropy of ρ_{AB} , the joint state of systems A and B . Let A , B and C correspond to three adjacent blocks of our translational invariant spin chain, with M , $L-M$ and M spins respectively. Then we have

$$S(ABC) = S_{L+M} \quad (2.10)$$

$$S(AB) = S(BC) = S_L \quad (2.11)$$

$$S(B) = S_{L-M}, \quad (2.12)$$

and Eq. (2.9) reads

$$S_{L+M} + S_{L-M} \leq 2S_L, \quad (2.13)$$

from where Eq. (2.8) follows.

Finally, we note that the above properties imply that S_L does not decrease as a function of L in the interval $L \in [0, N/2]$. In particular, in the limit of an infinite chain, $N \rightarrow \infty$, S_L becomes a non-decreasing, concave function for all finite values of L .

2. Examples

It is possible to get extra insight into the properties of S_L as a measure of entanglement by analyzing some particular cases, as illustrated in figure 2. We note first that S_L is upper bounded by

$$S_L \leq \min\{L, N-L\}, \quad (2.14)$$

since ρ_L is supported in a local space of dimension $d_L = \min\{2^L, 2^{N-L}\}$, whereas S_L vanishes for all L only for product states.

The paradigmatic GHZ state of N spins or qubits,

$$\frac{1}{\sqrt{2}}(|0\rangle^{\otimes N} + |1\rangle^{\otimes N}), \quad (2.15)$$

is often regarded as a maximally entangled state. However, from the present perspective it is only slightly entangled. Indeed, the entropies of a block of spins are

$S_L = 1$ for $L = 1, \dots, N-1$, and are therefore far below the upper bound (2.14).

Here we will be concerned with spin-chain ground states that are invariant under translations (for a finite chain, we will assume that the extremal spins are connected and will require invariance under circular translations). One may wonder if this symmetry implies an extra restriction on the range of S_L . However, explicit examples of translationally invariant states have been found [36] that saturate the above upper bound. This is in contrast with the case of states that are invariant under all possible permutations of the spins. There the dimension $d_L^{\text{sym}} = L+1$ of the symmetric subspace leads to the upper bound $S_L^{\text{sym}} \leq \log_2 L + 1$.

Finally, at a critical point the ground state may have some extra symmetries. In particular, it is known that in the large scale limit (that is, for scales much larger than the distance between neighboring spins) a critical spin chain is *conformal invariant*. We will explore the implications of this additional symmetry in section VI. The ground state entropy for critical chains will turn out to grow as $S_L = k \log_2 L$ for some universal constant k .

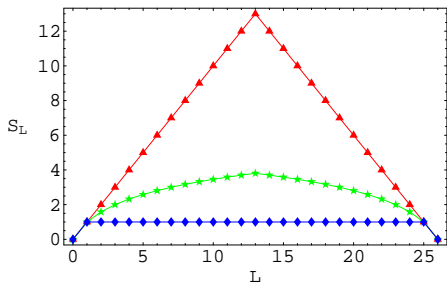


Figure 2: Different bounds for the entropy associated to different states in a system with $N=26$ spins. The triangles are the points for the linear bound in a 1D translational invariant state, which also apply to arbitrary n -qubit pure states. The stars are the logarithmic bound for a symmetric state under permutations. The diamonds are the values of the entropy for a GHZ state that is equal to one bit.

3. Majorization and von Neumann entropy

As mentioned above, the entanglement between a block of spins and the rest of the chain depends on the spectrum of the reduced density matrix ρ_L . Our ultimate aim is to characterize how this entanglement depends on the number L of spins in the block, hoping that this will allow us to capture, for instance, the emergence of criticality at quantum phase transition. We would like, therefore, to compare the spectrum of ρ_L for different values of L .

The entropy S_L can be used for this purpose, for it establishes an order in the set of probability distributions (equivalently, the set of spectra of density matrices). For instance, we have mentioned above that the entropy S_L

is non-decreasing in the interval $L \in [0, N/2]$. We can then use this result to say that, according to the entropy, the entanglement of a block of spins and the rest of the chain monotonically increases with the size of the block (for blocks smaller than half of the chain).

Nevertheless, there are other powerful tools to compare probability distributions, and by using them one may obtain a finer characterization of entanglement. In particular, a far more tight sense of (partial) ordering between probability distributions is established by Majorization theory [37, 38].

Let us recall that a given probability distribution $\{x_i\}$, where $x_1 \geq \dots \geq x_n$, is majorized by another probability distribution $\{y_i\}$, where $y_1 \geq \dots \geq y_n$, denoted $x \prec y$, when

$$\begin{aligned} x_1 &\leq y_1 \\ x_1 + x_2 &\leq y_1 + y_2 \\ x_1 + x_2 + \dots + x_n &= y_1 + y_2 + \dots + y_n, \end{aligned} \quad (2.16)$$

and that $x \prec y$ expresses the fact that x is *more disordered* than y . Given two arbitrary probability distributions x and y , the set of inequalities (2.16) are not likely to be fulfilled, but when they are, most measures of order are consistent with $x \prec y$. In particular, the von Neumann entropy fulfills

$$\rho \prec \rho' \Rightarrow S(\rho) > S(\rho'), \quad (2.17)$$

where $\rho \prec \rho'$ refers to majorization between the spectra of these two density matrices.

We shall later explore whether a majorization relation underlies the scaling behavior of the entropy S_L at critical points.

C. Entanglement in numerical studies of a spin chain

There are many aspects of the ground state of a spin chain that could be taken as a guide to characterize its entanglement. Our particular choice is mainly motivated by the role the reduced density matrix of a block of spins plays in some numerical schemes.

White's density matrix renormalization group (DMRG) method is a numerical technique that has brought an enormous progress in the study of one-dimensional quantum systems such as quantum spin chains [22]. It allows to compute ground-state energies and correlation functions with spectacular accuracy for non-critical spin chains, but it loses its grip (as many other methods) near a critical point. The method fails to work for quantum spin lattices in two or three dimensions [23] even away from the critical point. As recently explained by Osborne and Nielsen [39] in the language of quantum information, the degree of performance of this method is directly related to the way it accounts for entanglement.

The method is based on computing properties of the ground state $|\Psi_g\rangle$ of, say, a spin chain by constructing an approximation to the reduced density matrix ρ_L for a block of L spins, for an increasing value of L . This is done by retaining only the relevant degrees of freedom from the Hilbert space associated to the spin-block, as given by the eigenvectors of ρ_L with greatest weights or eigenvalues p_L^i . The spectrum $\{p_L^i\}_{i=1}^{\chi_L}$ of ρ_L ($\sum_{i=1}^{\chi_L} p_L^i = 1$) determines how many of these eigenvectors have to be retained in order to achieve a given accuracy in the calculations. A very spread spectrum (roughly equivalent to a lot of entanglement between the block of spins and the rest of the chain) will imply that many eigenvalues have to be retained, which translates into an increase in the computational cost of the calculation.

Therefore, by studying the spectrum of ρ_L , and in particular the rank χ_L of ρ_L , we may be able to assess how well the DMRG will perform for given values of the parameters (external magnetic field, spin-spin interaction) defining a particular spin model. In practice, the density matrix ρ_L may develop many small eigenvalues whose overall contribution is negligible given the required accuracy in the calculations. In this case it is more convenient to use an effective rank χ_L^{eff} , such that $\sum_{i=1}^{\chi_L^{\text{eff}}} p_L^i$ is sufficiently close to 1, where we assume that the eigenvalues are decreasingly ordered.

Relatedly, the rank χ_L (or the effective rank χ_L^{eff}) appears also as a decisive parameter in a recently proposed numerical scheme for the classical simulation of quantum spin chains [8]. In this scheme the cost of the simulation is linear in the number N of spins in the chain and grows as a small polynomial in χ ,

$$\chi \equiv \max_L \chi_L, \quad (2.18)$$

that is, in the maximal rank achieved for blocks of adjacent spins.

In summary, analyzing the spectrum of ρ_L , and in particular its rank χ_L (or χ_L^{eff}) is of direct interest for the numerical study of spin chains. The entropy S_L of ρ_L naturally appears as an estimator of the rank χ_L . Indeed, we have

$$\chi_L \geq 2^{S_L}. \quad (2.19)$$

In particular, a saturation of S_L as a function of L will turn out to indicate that χ_L^{eff} achieves also a maximum value—and therefore the chain can be efficiently simulated. In turn, if S_L unboundedly grows with L , then so does χ_L^{eff} , directly affecting the degree of calculational accuracy the above methods can achieve.

Note added: after completing the present work we have become aware of a number of contributions that study the spectrum of the reduced density matrix ρ_L also with a view to assess the performance of the DMRG [40].

III. XY MODEL

This section is devoted to study the entanglement of an infinite XY spin chain. We start by reviewing the main features of the XY model and by identifying the regions, in the space of parameters defining the model, where the spin chain becomes critical. Then, we compute the ground state $|\Psi_g\rangle$ of the system, from which we obtain the reduced density matrix ρ_L for L contiguous spins. The knowledge of the eigenvalues of ρ_L allows us to compute its entropy S_L and, therefore, have a quantification of entanglement in spin chains. Further information contained in the eigenvalues of the density matrix will be explored in the last section.

A. The XY Hamiltonian

The XY model consists of a chain of N spins with nearest neighbor interactions and an external magnetic field, as given by the Hamiltonian

$$H_{XY} = -\sum_l \left(\frac{1+\gamma}{2} \sigma_l^x \sigma_{l+1}^x + \frac{1-\gamma}{2} \sigma_l^y \sigma_{l+1}^y + \lambda \sigma_l^z \right). \quad (3.1)$$

Here l labels the N spins, σ_l^μ ($\mu = x, y, z$) are the Pauli matrices,

$$\sigma^x = \begin{pmatrix} 0 & 1 \\ 1 & 0 \end{pmatrix}, \quad \sigma^y = \begin{pmatrix} 0 & -i \\ i & 0 \end{pmatrix}, \quad \sigma^z = \begin{pmatrix} 1 & 0 \\ 0 & -1 \end{pmatrix}, \quad (3.2)$$

acting on spin l , with

$$[\sigma_l^\mu, \sigma_m^\nu] = 2i\delta_{lm} \sum_{\tau=x,y,z} \epsilon_{\mu\nu\tau} \sigma_l^\tau, \quad (3.3)$$

whereas parameter λ is the intensity of the magnetic field, applied in the Z direction, and parameter γ determines the degree of anisotropy of spin-spin interaction, which is restricted to the XY plane in spin space.

The XY model encompasses two other well-known spin models. If the interaction is restricted to the X direction in spin space, that is $\gamma = 1$, then H_{XY} turns into the Ising Hamiltonian with transverse magnetic field,

$$H_{\text{Ising}} = -\sum_l (\sigma_l^x \sigma_{l+1}^x + \lambda \sigma_l^z). \quad (3.4)$$

If, instead, we consider the interaction to be isotropic in the XY plane, $\gamma = 0$, then we recover the XX Hamiltonian with transverse magnetic field,

$$H_{XX} = -\sum_l \left(\frac{1}{2} [\sigma_l^x \sigma_{l+1}^x + \sigma_l^y \sigma_{l+1}^y] + \lambda \sigma_l^z \right). \quad (3.5)$$

We note that these Hamiltonians are used to model the physics of one dimensional arrays of spins, but also to describe other quantum phenomena. For instance, the

XX Hamiltonian corresponds to a particular limit of the boson Hubbard model

$$H_B = \sum_l \left(-w[\check{a}_l^\dagger \check{a}_{l+1} + \check{a}_l^\dagger \check{a}_{l+1}] - \mu n_l + \frac{U}{2} n_l(n_l - 1) \right),$$

where \check{a} are bosonic annihilation operators,

$$[\check{a}_l, \check{a}_m^\dagger] = \delta_{lm}, \quad (3.6)$$

and $n_l \equiv \check{a}_l^\dagger \check{a}_l$ are number operators. The boson Hubbard model (see chapters 10 and 11 of [7]) consists of spinless bosons on N sites, representing, say, Cooper pairs of electrons undergoing Josephson tunneling between superconducting islands or helium atoms moving on a substrate. The first term in H_B , proportional to w , allows hopping of bosons from site to site. The second term determines the total number of bosons in the model, with μ the chemical potential. The last term, with $U > 0$, is a repulsive on-site interaction between bosons. Now, in the limit of large U , no more than 1 boson will be present at each site. Thus, each of the N sites has an effective two-dimensional local space, and the identification

$$\sigma_l^x = \check{a}_l + \check{a}_l^\dagger, \quad (3.7)$$

$$\sigma_l^y = -i(\check{a}_l - \check{a}_l^\dagger), \quad (3.8)$$

$$\sigma_l^z = 1 - 2\check{a}_l^\dagger \check{a}_l, \quad (3.9)$$

takes H_B into

$$H_B^{U \rightarrow \infty} = -\sum_l \left(\frac{w}{2} [\sigma_l^x \sigma_{l+1}^x + \sigma_l^y \sigma_{l+1}^y] - \frac{\mu}{2} \sigma_l^z \right), \quad (3.10)$$

which is the Hamiltonian of the XX spin chain model with transverse magnetic field of Eq (3.5).

B. Spectrum of H_{XY} and critical properties

In appendix A we show that the spectrum of Hamiltonian H_{XY} in Eq. (3.1) is given, in the limit of large N , by

$$\Lambda_\phi = \sqrt{(\lambda - \cos \phi)^2 + \gamma^2 \sin^2 \phi}, \quad (3.11)$$

where $\phi \in [-\pi, \pi]$ is a label in momentum space. We can use the explicit expression (3.11) of Λ_ϕ to discuss the appearance of critical behavior in the XY model as a function of parameters (γ, λ) .

The correlation length ξ characterizes the exponential decay of correlations in the spin chain [42, 43],

$$\langle \sigma_l^a \sigma_{l+L}^b \rangle - \langle \sigma_l^a \rangle \langle \sigma_{l+L}^b \rangle \sim \exp(-L/\xi), \quad (3.12)$$

whereas the low energy dispersion Δ is given by

$$\Delta \equiv \Lambda_{\phi=0}. \quad (3.13)$$

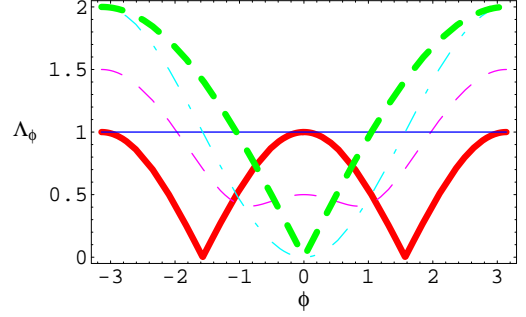


Figure 3: Energy of the system for different values of the parameters λ and γ as a function of ϕ . The thick plot corresponds to the XX model without magnetic field, the dashed one to a system with $\lambda = \gamma = 0.5$, the flat one is the Ising limit without magnetic field and the dot-dashed one and the thick dashed plot correspond to the isotropic and Ising model with $\lambda = 1$, respectively.

The critical scaling of these two quantities is characterized in terms of $|\lambda - \lambda_c|$ (deviation from the critical magnetic field λ_c) and critical exponents ν and s through

$$\begin{aligned} \xi &\sim |\lambda - \lambda_c|^{-\nu}, \\ \Delta &\sim |\lambda - \lambda_c|^s. \end{aligned} \quad (3.14)$$

In addition, the dynamical critical behavior is given by the energy dispersion,

$$\Lambda_{\phi \rightarrow 0} \sim \phi^z (1 + (\phi \xi)^{-z}), \quad (3.15)$$

where z is the dynamical exponent. An analysis of the scaling phenomena gives the following useful relation between the critical exponents: $z = s/\nu$.

For $\lambda = 1$ and any value of the anisotropy $\gamma \in [0, 1]$, the spectrum Λ_ϕ in Eq. (3.11) has no mass gap, $\Delta = 0$, and the spin chain is critical, so that $\lambda_c = 1$. As far as criticality is concerned, we need to distinguish two cases depending on the anisotropy γ .

(i) For $\gamma \in (0, 1]$, Eq. (3.11) implies that the behavior for the energy dispersions are

$$\begin{aligned} \Delta &= \Lambda_{\phi=0} = |\lambda - 1|, \\ \Lambda_{\phi \rightarrow 0} &\sim \sqrt{(\lambda - 1)^2 + (\gamma^2 + 1 - \lambda)\phi^2} \\ &\sim \phi \left(1 + \frac{|\lambda - 1|}{\phi} \right). \end{aligned} \quad (3.16)$$

At the critical point $\lambda_c = 1$, we find the critical exponents $z = 1$ and $s = 1$, whereas the divergence of the correlation length in this interval is

$$\xi = \frac{1}{|\lambda - 1|}, \quad (3.17)$$

with a critical exponent $\nu = 1$. For later reference, we state that in this case the quantum spin chain belongs to the same *universality class* as the classical Ising model in

two dimensions (or quantum Ising model in one dimension). The critical behavior in this class is described by the *conformal field theory* of a free massless fermion in 1+1 dimensions, with *central charge* equal to 1/2.

(ii) For the case $\gamma = 0$, we have

$$\Lambda_\phi = |\lambda - \cos \phi| \quad (3.18)$$

and the long wave dispersion and the energy dispersion are

$$\begin{aligned} \Delta &= \Lambda_{\phi=0} = |\lambda - 1|, \\ \Lambda_{\phi \rightarrow 0} &\sim |\lambda - 1 + \phi^2/2| \\ &\sim \phi^2 \left| 1 + \frac{\lambda - 1}{\phi^2} \right|. \end{aligned} \quad (3.19)$$

Therefore the critical point $\lambda_c = 1$ leads to the critical exponent $z = 2$ and $s = 1$ and the divergence of the correlation length in this interval is

$$\xi = \frac{1}{\sqrt{\lambda - 1}}, \quad (3.20)$$

with a critical exponent $\nu = \frac{1}{2}$. Notice, however, that in this case the spectrum Λ_ϕ is gapless for any $\lambda \in [0, 1]$, since Λ_ϕ continuously vanishes for $\phi = \arccos(\lambda)$. This implies that the spin chain is actually critical for any value $\lambda \in [0, 1]$ of the magnetic field. Again for later reference, we mention that in this case the quantum spin chain belongs to the *universality class* described by a free massless boson in 1+1 dimensions. This conformal theory has *central charge* equal to 1.

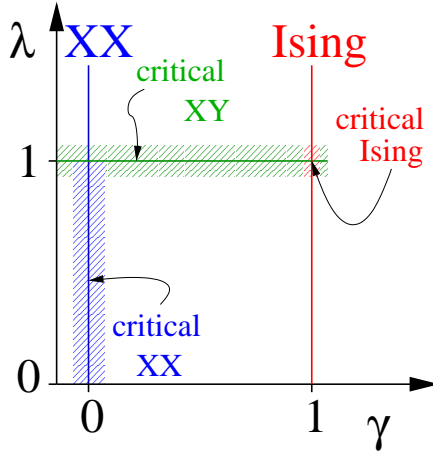


Figure 4: Critical regions in the parameter space (γ, λ) for the XY model. The Ising model, $\gamma = 1$, has a critical point at $\lambda = 1$. The XX model, $\gamma = 0$, is critical in the interval $\lambda \in [0, 1]$. The whole line $\lambda = 1$ is also critical.

Summarizing, there are two distinct critical regions in the parameter space (γ, λ) , namely the line $\lambda_c = 1$ and the segment $(\gamma, \lambda) = (1, [0, 1])$. The critical XX model corresponds to an unstable fixed point with respect to the anisotropy γ . If we depart from $(\gamma, \lambda) = (0, 1)$ by

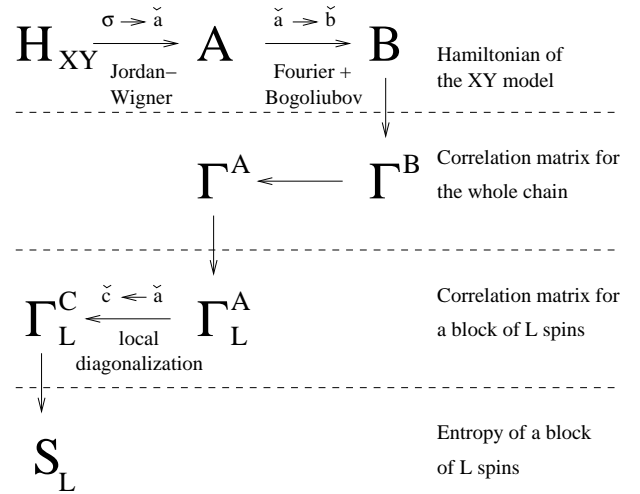


Figure 5: This road map describes the steps followed in order to obtain the entropy S_L of L contiguous spins from an infinite XY chain. We diagonalize the Hamiltonian H_{XY} by rewriting it first in terms of Majorana operators \check{a} and then in terms of Majorana operators \check{b} . The ground state $|\Psi_g\rangle$ is characterized by a correlation matrix Γ^B for operators \check{b} , Γ^A for operators \check{a} . Correlation matrix Γ_L^A describes the reduced density matrix ρ_L for a block of L spins. S_L is finally obtained from Γ_L^C , the block-diagonal form of Γ_L^A .

a small perturbation $\gamma \neq 0$, the critical behavior of the spin chain turns from the universality class of the *XX* model into that of the Ising model.

C. The ground state

We now turn to determine the ground state $|\Psi_g\rangle$ of the XY model with open boundary conditions,

$$\begin{aligned} H_{XY} = & - \sum_{l=-\frac{N}{2}+1}^{\frac{N}{2}-1} \left(\frac{1+\gamma}{2} \sigma_l^x \sigma_{l+1}^x + \frac{1-\gamma}{2} \sigma_l^y \sigma_{l+1}^y \right) \\ & - \sum_{l=-\frac{N}{2}+1}^{\frac{N}{2}} \lambda \sigma_l^z, \end{aligned} \quad (3.21)$$

in the limiting case of an infinite chain, $N \rightarrow \infty$. Through a Jordan-Wigner transformation, Hamiltonian H_{XY} can be cast into a quadratic form of fermionic operators, which in turn can be diagonalized by means of two additional canonical transformations, namely a Fourier transformation and a Bogoliubov transformation (see Appendix A for details). Next we will determine the ground state $|\Psi_g\rangle$ through a more convenient—although essentially equivalent—procedure that uses Majorana operators instead of fermionic operators. This calculation was sketched in [9] and uses the formalism described in [41].

1. Majorana operators

For each site l of the N -spin chain, we consider two Majorana operators, \check{a}_{2l-1} and \check{a}_{2l} , defined by

$$\check{a}_{2l-1} \equiv \left(\prod_{m < l} \sigma_m^z \right) \sigma_l^x; \quad \check{a}_{2l} \equiv \left(\prod_{m < l} \sigma_m^z \right) \sigma_l^y. \quad (3.22)$$

Operators \check{a}_m are Hermitian and obey anti-commutation relations,

$$\check{a}_m^\dagger = \check{a}_m, \quad \{\check{a}_m, \check{a}_n\} = 2\delta_{mn}. \quad (3.23)$$

The change of variables of Eq. (3.22), parallel to the Jordan-Wigner transformation described in Appendix A, implies

$$\check{a}_{2l}\check{a}_{2l+1} = \sigma_l^y \sigma_l^z \sigma_{l+1}^x = i\sigma_l^x \sigma_{l+1}^x, \quad (3.24)$$

$$\check{a}_{2l-1}\check{a}_{2l+2} = \sigma_l^x \sigma_l^z \sigma_{l+1}^y = -i\sigma_l^y \sigma_{l+1}^y, \quad (3.25)$$

$$\check{a}_{2l-1}\check{a}_{2l} = \sigma_l^x \sigma_l^y = i\sigma_l^z, \quad (3.26)$$

so that Hamiltonian H_{XY} becomes

$$\begin{aligned} H_{XY} = & i \sum_{l=-\frac{N}{2}+1}^{\frac{N}{2}-1} \left(\frac{1+\gamma}{2} \check{a}_{2l}\check{a}_{2l+1} - \frac{1-\gamma}{2} \check{a}_{2l-1}\check{a}_{2l+2} \right) \\ & + i \sum_{l=-\frac{N}{2}+1}^{\frac{N}{2}} \lambda \check{a}_{2l-1}\check{a}_{2l}, \end{aligned} \quad (3.27)$$

or, equivalently,

$$H_{XY} = \frac{i}{4} \sum_{m,n=-N+1}^N A_{mn} \check{a}_m \check{a}_n, \quad (3.28)$$

where A is a real, skew-symmetric matrix given by

$$A = \begin{bmatrix} A_0 & A_1 & & & \\ -A_1^T & A_0 & A_1 & & \\ & \ddots & & & \\ & & -A_1^T & A_0 & A_1 \\ & & & -A_1^T & A_0 \end{bmatrix}, \quad (3.29)$$

and

$$A_0 = \begin{bmatrix} 0 & 2\lambda \\ -2\lambda & 0 \end{bmatrix}, \quad A_1 = \begin{bmatrix} 0 & -(1-\gamma) \\ 1+\gamma & 0 \end{bmatrix}. \quad (3.30)$$

Let $W \in SO(2N)$ be a special orthogonal matrix that brings A into its block diagonal form $B = WAW^T$,

$$B = \bigoplus_{k=-\frac{N}{2}+1}^{\frac{N}{2}} \tilde{\Lambda}_k \begin{bmatrix} 0 & 1 \\ -1 & 0 \end{bmatrix}, \quad (3.31)$$

and let

$$\check{b}_p = \sum_{m=-N+1}^N W_{pm} \check{a}_m, \quad -N+1 \leq p \leq N, \quad (3.32)$$

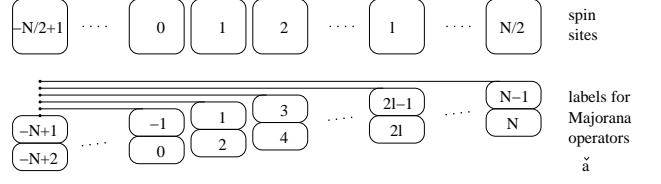


Figure 6: Through transformation (3.22), we can associate two Majorana operators, \check{a}_{2l-1} and \check{a}_{2l} , to site l of the spin chain. Notice, however, the non-local character of such transformation: \check{a}_{2l-1} and \check{a}_{2l} are a product of Pauli matrices from sites $-N/2+1$ to l .

be a new set of Majorana operators,

$$\check{b}_p^\dagger = \check{b}_p, \quad \{\check{b}_p, \check{b}_q\} = 2\delta_{pq}. \quad (3.33)$$

The canonical transformation induced by W is parallel to the Fourier and Bogoliubov transformations for fermionic operators that appear in Appendix A, where also an explicit expression for $\tilde{\Lambda}_k$ is displayed. In terms of operators \check{b} , H_{XY} reads

$$H_{XY} = \frac{i}{4} \sum_{p,q=-N+1}^N B_{pq} \check{b}_p \check{b}_q \quad (3.34)$$

$$= \frac{i}{4} \sum_{k=-\frac{N}{2}+1}^{\frac{N}{2}} \tilde{\Lambda}_k (\check{b}_{2k-1} \check{b}_{2k} - \check{b}_{2k} \check{b}_{2k-1}). \quad (3.35)$$

2. Correlation matrix

The diagonalization of H_{XY} essentially concludes with the determination of the explicit form of matrix W , as presented in Appendix B. However, in order to analyze the resulting ground state $|\Psi_g\rangle$, it is convenient to momentarily switch to the more familiar language of fermionic operators. We define a set of N spinless fermionic operators \hat{b} ,

$$\hat{b}_k \equiv \frac{\check{b}_{2k-1} + i\check{b}_{2k}}{2}, \quad (3.36)$$

$-N/2 \leq k \leq N/2-1$, obeying the anticommutation relations

$$\{\hat{b}_k^\dagger, \hat{b}_p\} = \delta_{kp}, \quad \{\hat{b}_k, \hat{b}_p\} = 0, \quad (3.37)$$

in terms of which Hamiltonian H_{XY} becomes, up to an irrelevant constant,

$$H_{XY} = \sum_{k=-\frac{N}{2}+1}^{\frac{N}{2}} \tilde{\Lambda}_k \hat{b}_k^\dagger \hat{b}_k. \quad (3.38)$$

The ground state of H_{XY} is annihilated by all \hat{b} ,

$$\hat{b}_k |\Psi_g\rangle = 0, \quad (3.39)$$

so that $\langle \Psi_g | \hat{b}_k^\dagger \hat{b}_k | \Psi_g \rangle$ —that is, the expectation value of a positive operator— vanishes and $\langle \Psi_g | H_{XY} | \Psi_g \rangle = 0$ corresponds to the smallest eigenvalue of H_{XY} . Then, since $\hat{b}_k^\dagger \hat{b}_k + \hat{b}_k \hat{b}_k^\dagger = I$ and $\hat{b}_k^\dagger \hat{b}_k | \Psi_g \rangle = 0$, we also have

$$\hat{b}_k \hat{b}_k^\dagger | \Psi_g \rangle = | \Psi_g \rangle. \quad (3.40)$$

Let $\langle M \rangle$ denote the expectation value $\langle \Psi_g | M | \Psi_g \rangle$ for operator M . We readily have

$$\langle \hat{b}_k \rangle = 0, \quad (3.41)$$

$$\langle \hat{b}_k \hat{b}_p \rangle = 0, \quad (3.42)$$

$$\langle \hat{b}_k \hat{b}_p^\dagger \rangle = \delta_{kp}. \quad (3.43)$$

More generally, Wick's theorem establishes that any non-vanishing expectation value corresponding to a product of operators \hat{b} and \hat{b}^\dagger can be expressed in terms of $\langle \hat{b}_k \hat{b}_p^\dagger \rangle$ and $\langle \hat{b}_k \hat{b}_p \rangle$ and their complex conjugates. For instance, we have

$$\begin{aligned} \langle \hat{b}_{k_1} \hat{b}_{k_2} \hat{b}_{k_3}^\dagger \hat{b}_{k_4}^\dagger \rangle &= \langle \hat{b}_{k_1} \hat{b}_{k_2} \rangle \langle \hat{b}_{k_3}^\dagger \hat{b}_{k_4}^\dagger \rangle - \langle \hat{b}_{k_1} \hat{b}_{k_3}^\dagger \rangle \langle \hat{b}_{k_2} \hat{b}_{k_4}^\dagger \rangle \\ &+ \langle \hat{b}_{k_1} \hat{b}_{k_4}^\dagger \rangle \langle \hat{b}_{k_2} \hat{b}_{k_3}^\dagger \rangle. \end{aligned} \quad (3.44)$$

This means that $|\Psi_g\rangle$ is a *gaussian state*, completely characterized by the expectation values of the first and second moments, Eqs. (3.41)-(3.43).

We can now return to the Majorana operators \check{b} . An equivalent characterization of $|\Psi_g\rangle$ is given in terms of the correlation matrix $\langle \check{b}_p \check{b}_q \rangle = \delta_{pq} + i\Gamma_{pq}^B$, where

$$\Gamma^B = \bigoplus_{k=-\frac{N}{2}+1}^{\frac{N}{2}} \begin{bmatrix} 0 & 1 \\ -1 & 0 \end{bmatrix}. \quad (3.45)$$

As direct substitution shows, Γ^B amounts for both the expectation values $\langle \hat{b}_k \hat{b}_p^\dagger \rangle$ and $\langle \hat{b}_k \hat{b}_p \rangle$ simultaneously, which is the ultimate reason to conduct the present derivation in terms of Majorana operators.

Finally, we use Γ^B to obtain the correlation matrix $\langle \check{a}_m \check{a}_n \rangle = \delta_{m,n} + i\Gamma_{mn}^A$ of the original Majorana operators \check{a} , where $\Gamma^A = W^T \Gamma^B W$. As shown in Appendix B, one obtains

$$\Gamma^A = \begin{bmatrix} \Pi_0 & \Pi_1 & \dots & \Pi_{N-1} \\ -\Pi_1 & \Pi_0 & & \vdots \\ \vdots & \ddots & \ddots & \vdots \\ -\Pi_{N-1} & \dots & \dots & \Pi_0 \end{bmatrix}, \quad \Pi_l = \begin{bmatrix} 0 & g_l \\ -g_{-l} & 0 \end{bmatrix}, \quad (3.46)$$

with real coefficients g_l as given, in the limit of an infinite chain, $N \rightarrow \infty$, by

$$g_l = \frac{1}{2\pi} \int_0^{2\pi} d\phi e^{-il\phi} \frac{a \cos \phi - 1 - ia\gamma \sin \phi}{|a \cos \phi - 1 - ia\gamma \sin \phi|}. \quad (3.47)$$

We conclude that Eqs. (3.46)-(3.47) contain a complete characterization of the ground state $|\Psi_g\rangle$ of H_{XY} .

D. Entropy of a block of spins

The entropy of the reduced density matrix ρ for L adjacent spins,

$$S_L = -\text{tr}(\rho \log_2 \rho), \quad (3.48)$$

can be computed from Γ^A , Eq. (3.46), as follows.

In the limit of an infinite chain, the middle of the chain is fully translational invariant, in that the same ρ_L describes the state of any block of L contiguous spins. For notational convenience we choose the block to contain qubits $l = 1, \dots, L$. We can expand the density matrix ρ_L of the block as

$$\rho_L = 2^{-L} \sum_{\mu_1, \dots, \mu_L=0,x,y,z} \rho_{\mu_1 \dots \mu_L} \sigma_1^{\mu_1} \dots \sigma_L^{\mu_L}, \quad (3.49)$$

where coefficients $\rho_{\mu_1 \dots \mu_L}$ are given by

$$\rho_{\mu_1 \dots \mu_L} = \langle \sigma_1^{\mu_1} \dots \sigma_L^{\mu_L} \rangle. \quad (3.50)$$

In spite of the non-local character of transformation (3.22), the density matrix ρ_L can be reconstructed from the restricted $2L \times 2L$ correlation matrix

$$\langle \check{a}_m \check{a}_n \rangle = \delta_{mn} + i\Gamma_L^A_{mn}, \quad m, n = 1, \dots, 2L, \quad (3.51)$$

where

$$\Gamma_L^A = \begin{bmatrix} \Pi_0 & \Pi_1 & \dots & \Pi_{L-1} \\ -\Pi_1 & \Pi_0 & & \vdots \\ \vdots & \ddots & \ddots & \vdots \\ -\Pi_{L-1} & \dots & \dots & \Pi_0 \end{bmatrix}. \quad (3.52)$$

Indeed, the symmetry

$$\left(\prod_l \sigma_l^z \right) H_{XY} \left(\prod_l \sigma_l^z \right) = H_{XY} \quad (3.53)$$

implies that $\rho_{\mu_1 \dots \mu_L} = 0$ whenever the sum of μ 's equal to x and of μ 's equal to y is odd. For instance, for $L = 4$, terms such as ρ_{0x0z} and ρ_{xy0y} vanish. Therefore non-vanishing coefficients $\rho_{\mu_1 \dots \mu_L}$ correspond to the expectation value of a product of Pauli matrices with an even total number of σ_x 's and σ_y 's. Such products are mapped through the inverse of transformation (3.22) into a product of an even number of Majorana operators \check{a}_m , with $m \in [1, 2L]$. (See Eqs. (3.24)-(3.26) for an example). We can then use Wick's theorem to express such products in terms of the second moments $\langle \check{a}_m \check{a}_n \rangle$, $m, n \in [1, 2L]$, all of which are contained in Γ_L^A .

In principle, then, one could use Γ_L^A , Wick's theorem and the inverse of transformation (3.22) to compute ρ_L , and extract S_L from its spectral decomposition. However, the spectrum of ρ_L , and its entropy S_L , can be computed in a more direct way from Γ_L^A .

Let $V \in SO(2L)$ be such that it brings Γ_L^A into its block-diagonal form $\Gamma_L^C = V\Gamma_L^AV^T$,

$$\Gamma_L^C = \bigoplus_{l=1}^L \begin{bmatrix} 0 & \nu_l \\ -\nu_l & 0 \end{bmatrix}. \quad (3.54)$$

Matrix V defines a set of $2L$ Majorana operators

$$\check{c}_m \equiv \sum_{n=1}^{2L} V_{mn} \check{a}_n, \quad (3.55)$$

with correlation matrix $\langle \check{c}_m \check{c}_n \rangle$ given by

$$\langle \check{c}_m \check{c}_n \rangle = \delta_{mn} + i(\Gamma_L^C)_{mn}. \quad (3.56)$$

The structure of Γ_L^C implies that mode \check{c}_{2l-1} is only correlated to mode \check{c}_{2l} , a most convenient fact that we next exploit.

Again for the sake of clarity, we complete the present reasoning using a more familiar language of fermionic modes. We define L spinless fermionic operators

$$\hat{c}_l \equiv \frac{\check{c}_{2l-1} + i\check{c}_{2l}}{2}, \quad (3.57)$$

$$\{\hat{c}_l, \hat{c}_m\} = 0, \quad \{\hat{c}_l^\dagger, \hat{c}_m\} = \delta_{lm}. \quad (3.58)$$

By construction they fulfill

$$\langle \hat{c}_m \hat{c}_n \rangle = 0, \quad \langle \hat{c}_m^\dagger \hat{c}_n \rangle = \delta_{mn} \frac{1 + \nu_m}{2}, \quad (3.59)$$

which means that the L fermionic modes are uncorrelated, that is in a *product* state,

$$\rho_L = \varrho_1 \otimes \cdots \otimes \varrho_L. \quad (3.60)$$

[Notice that this tensor product structure does not correspond in general to a factorization into local Hilbert spaces for the L spins, but is instead a rather non-local structure]. The density matrix ϱ_l has eigenvalues

$$\frac{1 \pm \nu_l}{2} \quad (3.61)$$

and entropy

$$S(\varrho_l) = H_2 \left(\frac{1 + \nu_l}{2} \right), \quad (3.62)$$

where $H_2(x) = -x \log x - (1-x) \log(1-x)$ denotes the binary entropy. The spectrum of ρ_L results now from the L -fold product of the spectra of the density matrices ϱ_l , and the entropy of ρ_L is the sum of entropies of the L uncorrelated modes,

$$S_L = \sum_{l=1}^L H_2 \left(\frac{1 + \nu_l}{2} \right). \quad (3.63)$$

Summarizing: for arbitrary values of the anisotropy γ and magnetic field λ , and in the thermodynamic limit

corresponding to an infinite chain ($N \rightarrow \infty$), the entropy S_L of the ground state of the XY model can in practice be obtained by (i) evaluating Eq. (3.47) numerically for $l = 0, \dots, L-1$, (ii) diagonalizing Γ_L^A in Eq. (3.52), so as to obtain ν_m , and (iii) evaluating S_L using Eq. (3.63). Appendix C contains an analytical expression of the coefficients g_l in Eq. (3.47) for several particular cases.

Scaling of the entropy

We can now proceed to compute the entropy for the XY model with different parameters. It is first important to note that the actual diagonalization to be performed takes place in a $2L \times 2L$ space, not in the huge $2^L \times 2^L$ space associated to the vacuum density matrix. This is obvious in Fig. (7) where the computation can easily include hundreds of spins.

The result obtained for the reduced density matrix of L spins in the isotropic XX model, $\gamma = 0$, with no external magnetic field, $\lambda = 0$, perfectly fits a logarithmic behavior

$$S_L^{XX} = \frac{1}{3} \log_2 L + a \quad \gamma = 0, \lambda = 0, \quad (3.64)$$

where a is a constant close to $\pi/3$. This result shows that entanglement of the vacuum state scales at this critical point, pervading the whole system and carefully organizing the complicate superposition of states that will wind up reproducing correlators. The scaling of entanglement, furthermore follows some universality properties we shall discuss later.

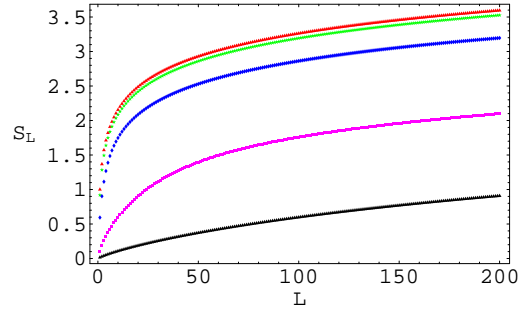


Figure 7: Entropy of the reduced density matrix for L spins in the isotropic XX model, $\gamma = 0$, with different external magnetic field λ . The maximum entropy is reached when there is no applied external field. The entropy decreases while the magnetic field increases until $\lambda = 1$ when the system reaches the ferromagnetic limit and the ground state is a product state in the spin basis.

It is easy to extend our computation to other critical and non-critical points in the parameter space for the XY

system. Fig. (8) shows the scaling of entanglement as we scan γ . Note again the logarithmic scaling of the entropy although its coefficient is now $1/6$ instead of $1/3$. The constant correction to the logarithmic scaling is such that

$$S_L^{XY} = \frac{1}{6} \log_2 L + a(\gamma), \quad (3.65)$$

so that

$$\lim_{L \rightarrow \infty} [S_L(\gamma = 1) - S_L(\gamma)] = -\frac{1}{6} \log_2 \gamma. \quad (3.66)$$

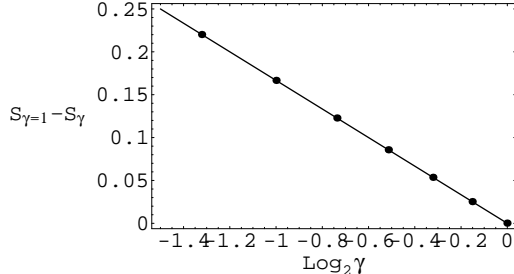


Figure 8: Difference of the entropy $\lim_{L \rightarrow \infty} [S_L(\gamma = 1) - S_L(\gamma)]$ for different values of the anisotropy γ . For every γ the model is critical and the entropy scales as $\frac{1}{6} \log_2 L + a(\gamma)$, where the L -independent function $a(\gamma)$ is perfectly fitted by $-\frac{1}{6} \log_2 \gamma$.

When $\gamma = 1$ the system is described by the Ising model. The entropy behavior in this limit can be viewed in the Fig. (9). When the magnetic field is turned to $\lambda = 1$ the entropy reproduces the scaling law

$$S_L^{Ising} = \frac{1}{6} \log_2 L + a \quad \gamma = 1, \lambda = 1. \quad (3.67)$$

For the Ising model with no external field, the ground state that minimizes the total energy is the Néel state, a macroscopic GHZ state, for which the entropy is always equal to one.

IV. HEISENBERG MODEL

A. The Hamiltonian

The Heisenberg interaction can be obtained from the well known fermion Hubbard model,

$$H = \sum_{i\sigma} \left(\epsilon_0 \hat{h}_{i\sigma}^\dagger \hat{h}_{i\sigma} + t(\hat{h}_{i\sigma}^\dagger \hat{h}_{i+1\sigma} + \hat{h}_{i+1\sigma}^\dagger \hat{h}_{i\sigma}) \right) + \sum_i U \hat{h}_{i\uparrow}^\dagger \hat{h}_{i\uparrow} \hat{h}_{i\downarrow}^\dagger \hat{h}_{i\downarrow}. \quad (4.1)$$

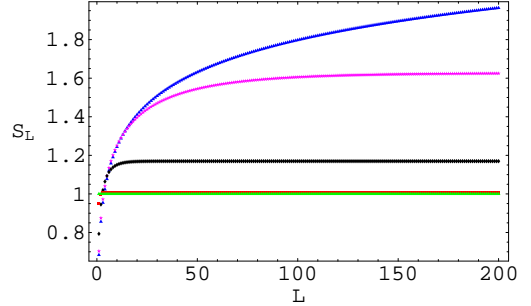


Figure 9: Entropy for the reduced density matrix to L spins of the Ising model, $\gamma = 1$, with different values of the external magnetic field, $\lambda \in \{0, 1\}$. The maximum entropy is reached at the critical point when the applied field is one. Other values of the magnetic field lead to saturation of the entropy. For a magnetic field $\lambda = 0$ the ground state of the system is in the Néel state or GHZ state.

This hamiltonian describes a chain of N electrons, with $\{\hat{h}_i\}$ and $\{\hat{h}_i^\dagger\}$ being annihilation and creation electron operators that anticommute, $\{\hat{h}_i^\dagger, \hat{h}_i\} = 1$, and the variable $\sigma = \{\uparrow, \downarrow\}$ corresponds to the spin orientation. Other parameters that define the model are the one particle interaction at the same site, ϵ_0 , the one particle interaction at different sites or tunneling parameter, t , and the two particles interactions that are simplified to two electrons interacting at the same site, U .

We can see that for this kind interactions, the higher the $|t|$ the better conductor is the system (just because t is the electron diffusion probability). When $U \gg t$, two electrons are not energetically allowed to be at the same site, and it is easy to obtain from the Hubbard model the Heisenberg limit. Defining the spin operators $S_i^z = \frac{1}{2}(\hat{h}_{i\uparrow}^\dagger \hat{h}_{i\uparrow} - \hat{h}_{i\downarrow}^\dagger \hat{h}_{i\downarrow})$, $S_i^+ = \hat{h}_{i\uparrow}^\dagger \hat{h}_{i\downarrow}$, $S_i^- = \hat{h}_{i\downarrow}^\dagger \hat{h}_{i\uparrow}$ the Hubbard model can be recast into

$$H = J \sum_i \vec{S}_i \vec{S}_{i+1}, \quad (4.2)$$

where $J = 4 \frac{t^2}{U}$. Metal-insulator transitions, superconductive systems or magnetic properties can be explained with this Hamiltonian. Note that ϵ_0 does not appear in a explicit way due to the fact that for any configuration and in the limit $U \gg t$ the term $\hat{h}_{i\sigma}^\dagger \hat{h}_{i\sigma}$ is a constant corresponding to the occupation number of the i -th site.

The general Heisenberg Hamiltonian with nearest neighbors interactions and a transverse magnetic field for spin- $\frac{1}{2}$ particles in a 1D ring is given by,

$$H = J \sum_{i=1}^N \left[\frac{1}{2} (S_i^+ S_{i+1}^- + S_i^- S_{i+1}^+) + \Delta S_i^z S_{i+1}^z \right] + \sum_{i=1}^N B^z S_i^z, \quad (4.3)$$

where J is the coupling constant and the parameter Δ is called *anisotropy* which evaluates the interaction

strength in the z -direction respect to the orthogonal one. The homogenous magnetic field, B^z , points to the z -direction. The operator \vec{S} are the $\frac{1}{2}$ -spin operators defined by the commutation relations:

$$[S_i^z, S_j^\pm] = \pm \delta_{ij} S_i^\pm, \quad [S_i^+, S_j^-] = 2\delta_{ij} S_i^z, \quad (4.4)$$

and with periodic boundary conditions,

$$S_{i+N}^\alpha = S_i^\alpha, \quad \alpha \in \{z, +, -\}, \quad i \leq N. \quad (4.5)$$

We can see that in the limit of $\Delta \rightarrow 0$ the system is in the XX model class with a transverse magnetic field.

To study the properties of entanglement in the parameter space of the Heisenberg hamiltonian we can make a separation of the type $H(\mathcal{K}) = H_0 + \mathcal{K}H_1$. In some interesting cases, \mathcal{K} is a dimensionless parameter \mathcal{K} and H_0 commutes with H_1 , so that both operators can be simultaneously diagonalized. For instance, \mathcal{K} may correspond in our model either to the anisotropy, Δ , or to the ratio between the magnetic field and the coupling constant between the spins, $B^z/J \equiv \lambda$. When the coupling \mathcal{K} is modified, the spectrum changes. In the case when an excited level decreases its energy enough to become the ground state, two levels must have crossed and a point of non-analyticity is created as a function of \mathcal{K} . Any point of non-analyticity in the system is identified as a *QPT*.

B. Bethe Ansatz for the Heisenberg model

Several properties make the Heisenberg Hamiltonian completely integrable. Two symmetries are essential to get the model solution and are used in the *Bethe Ansatz* (*BA*) [44]. (1) One is the rotational symmetry about the z -axis in spin space, which we have chosen to be the quantization axis, that implies that the z -component of the total spin S_T^z is conserved. Sorting the basis vectors according to the quantum number $S_T^z = N/2 - r$, where N is the number of sites in the chain and r the number of down spins, is all that is required to block diagonalize the Hamiltonian matrix. (2) The second symmetry is the invariance of H with respect to discrete translations by any number of lattice spacings. To reconstruct the whole spectrum of the Heisenberg model, Bethe's idea starts from the ferromagnetic state, F , to get a translational invariant eigenstate of the Hamiltonian with one unit of z -spin angular momentum less than the F state. The F state has the maximum value of the spin angular momentum, $\frac{N}{2}$, as all the spins in the chain are pointing to the magnetic field direction. The iteration of this process produces the spectrum of the Heisenberg model.

Here, we shall use the *BA* to get a numerical but exact solution of a finite spin chain. Finite size effects are present but can be controlled by comparing different sizes. Scaling of entanglement is thus approached asymptotically as the size grows. For a general S_T^z value, the main equations to solve the Heisenberg Hamiltonian

are,

$$|\Psi\rangle = \sum_{1 \leq n_1 < \dots < n_r \leq N} a(n_1, \dots, n_r) |n_1, \dots, n_r\rangle, \quad (4.6)$$

where $|n\rangle$ represents the n -th down-spin and the rest ones are up-spins and

$$a(n_1, \dots, n_r) = \sum_{\mathcal{P} \in \mathcal{S}_r} \exp \left(i \sum_{j=1}^r k_{\mathcal{P}j} n_j + \frac{i}{2} \sum_{i \leq j} \theta_{\mathcal{P}i, \mathcal{P}j} \right), \quad (4.7)$$

where $\mathcal{P} \in \mathcal{S}_r$ is the $r!$ permutations of $\{1, \dots, r\}$ and k_i and $\theta_{i,j}$ with $(i, j) \in \{1, \dots, r\}$ are the parameters to be determined.

Three general conditions hold for these parameters [45]:

$$\begin{aligned} \theta_{i,j} &= -\theta_{j,i} \quad \forall \{i, j\}, \\ \cot \frac{\theta_{i,j}}{2} &= \frac{\Delta \sin \frac{k_i - k_j}{2}}{\cos \frac{k_i + k_j}{2} + \Delta \cos \frac{k_i - k_j}{2}} \quad (i, j) \in \{1, \dots, r\}, \\ Nk_i &= 2\pi\lambda_i + \sum_{j \neq i} \theta_{i,j} \quad i \in \{1, \dots, r\}, \end{aligned} \quad (4.8)$$

where the integers λ_i are called Bethe quantum numbers. The states are completely determined by the Bethe quantum numbers and Eqs. (4.6)-(4.8).

It is known [46] that the set $\{\lambda_i\}$ with the lowest energy for each $S_T^z = N/2 - r$ satisfies:

$$\lambda_i = S_T^z - 1 + 2i = \frac{N}{2} - r - 1 + 2i \quad i \in \{1, \dots, r\}. \quad (4.9)$$

The expression for the ground state energy reads

$$E - E_F = -J \sum_{i=1}^r (\Delta - \cos k_i) + B^z S_T^z, \quad E_F = \frac{JN\Delta}{4}. \quad (4.10)$$

We have found convenient to solve the previous system of non-linear equations using a minimization code for absolute errors based on genetic algorithms, although many other numerical techniques could have been used. Precision can be controlled by setting a maximum bound in the numerical error in the parameters θ 's and k 's to 10^{-5} . This small error has proven enough to detect the scaling of entropy. The systems that we study have an even number of sites N , so the eigenvalue of the S_T^z operator in the ferromagnetic system is the integer $N/2$.

C. Entropy of a block of spins

The fact that the *BA* is used to compute numerically the eigenvalues of the reduced density matrix of blocks of spins limits the size of the system that can be studied. The results we obtain are thus less precise than those for

the XY model although scaling laws can be inferred with confidence. As a first step, we concentrate on the effect of the finite size system for the entropy results. More precisely, we analyze the isotropic model without magnetic field in a chain of $N = \{8, 10, 12, 14, 16, 18\}$ sites. The results are plotted in Fig.[10]. Finite size effects bend down the entropy when the size of the block approaches half of the chain. Smaller blocks are less sensitive to the finite size and show good scaling. The numerical results indicate that the entropy behavior converges to a logarithmic scaling when as the size of the system increases. This asymptotic behavior corresponds to

$$S_L \sim \frac{1}{3} \log_2 L. \quad (4.11)$$

Entropy scaling falls into the universality class of a free boson.

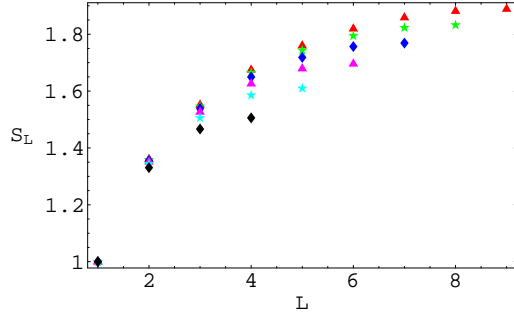


Figure 10: Dependence of the entropy on the finite size of the chain in a isotropic Heisenberg model without magnetic field. In the plot, triangles, stars, diamonds, triangles, stars and diamonds correspond to 18, 16, 14, 12, 10, and 8 spins chains, respectively.

1. Isotropic model in a magnetic field

The Heisenberg model can be perturbed in several different directions. We first introduce an external magnetic field while eliminating the anisotropy. This case corresponds to the hamiltonian

$$H' = \sum_{i=1}^N \left[\frac{1}{2} (S_i^+ S_{i+1}^- + S_i^- S_{i+1}^+) + S_i^z S_{i+1}^z \right] + \lambda \sum_{i=1}^N S_i^z, \quad (4.12)$$

where we have redefined the parameters in Eq.[4.3] as follows

$$H' = \frac{H}{J}, \quad \lambda = \frac{B^z}{J}, \quad , \quad (4.13)$$

and set $\Delta = 1$. We can now use the *BA* to compute the eigenstates of the Hamiltonian in the critical interval: $\lambda \in [0, 2]$ [47]. For values of $|\lambda|$ greater or equal to 2, every spin in the system is pointing in the magnetic field direction and the state is a product of S_i^z eigenstates. Entanglement has disappeared.

As implicit in the *BA*, the ground state has a well defined magnetization, S_T^z . This quantity changes every time the tuning of the magnetic field implies a new level-crossing. The relation between the magnetization, S_T^z , and the ratio λ between the magnetic field B^z and the coupling constant J is well defined and can be easily obtained from the spectrum of the model.

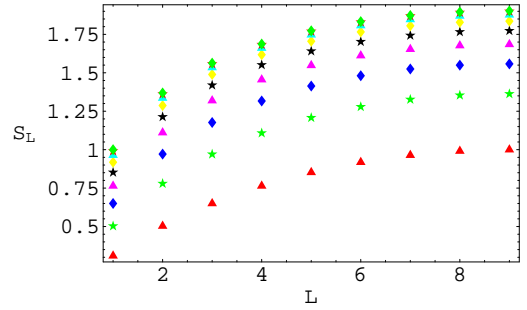


Figure 11: Entropy for blocks of size L in a $N = 18$ ring up to $L = N/2 = 9$ spins for different coupling values, $\lambda \in \{0, 0.24, 0.68, 1.05, 1.35, 1.59, 1.77, 1.89, 1.97\}$. The entropy remains constant in the interval between level crossing, but every time the coupling is at one of the latter points the entropy value changes. The maximum in the entropy is obtained for the antiferromagnetic system without magnetic field, while the entropy goes to zero for $\lambda \rightarrow 2$.

The Heisenberg model has two limiting behaviors. On the one hand, for $\lambda = 0$ ($B^z = 0$) the ground state is antiferromagnetic, with a null angular momentum eigenvalue. On the other hand, for $\lambda \geq 2$, the ground state of the system corresponds to the ferromagnetic state. Figs. [11] and [12] illustrate how the entropy of a finite spin ring changes when λ varies in the interval $[0, 2]$. Fig. [11] shows the way the entropy decreases as λ increases, obtaining the zero value when $\lambda \rightarrow 2$ where the ground state turns into a product state. The λ values that are plotted are those in which the ground state has a level crossing, $\{0, 0.24, 0.68, 1.05, 1.35, 1.59, 1.77, 1.89, 1.97\}$ for a ring with $N = 18$ sites. The entropy remains constant in the interval between level crossings, changing its value every time the coupling is at one of the latter coupling points. Fig. [12] plots the way the entropy increases logarithmically when λ decreases, keeping fixed the number of traced spins.

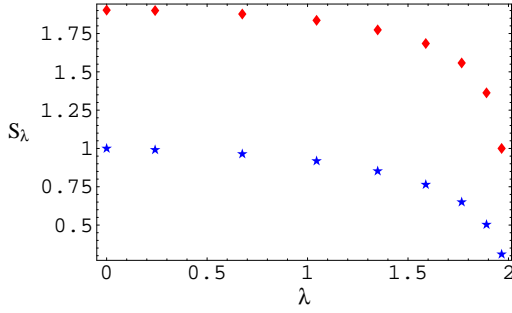


Figure 12: Entropy in a $N = 18$ spin rings for different λ values. Stars correspond to one traced site out and diamonds to $N/2 = 9$ traced spins.

2. Anisotropic model

It is of interest to analyze the behavior of entanglement for the deformation of the anisotropic Heisenberg chain and no external magnetic field, that is

$$H'' = \sum_{i=1}^N \left(\frac{1}{2} (S_i^+ S_{i+1}^- + S_i^- S_{i+1}^+) + \Delta S_i^z S_{i+1}^z \right), \quad (4.14)$$

which corresponds to a particular case of Eq. [4.3], taking

$$H'' = \frac{H}{J}, \quad B^z = 0. \quad (4.15)$$

In this case, the critical interval [48] corresponds to $\Delta \in [-1, 1]$. For $\Delta = 1$ we recover the isotropic antiferromagnetic model and, for the case $\Delta = -1$, the system turns into the isotropic ferromagnetic model. The sign in $(S_i^+ S_{i+1}^- + S_i^- S_{i+1}^+)$ does not change the eigenstates of the system but only their energy values. One model, e.g. with a positive sign, can be recast into the other, with opposite sign, applying a local π rotation respect to the z -axis in the first of every two contiguous spins. Entanglement remains invariant under this transformation. This argument shows that entanglement is a robust magnitude and depends on fewer details of the system than e.g. its magnetization.

The anisotropy is a marginal deformation in the interval $[-1, 1]$. Fig.[13] shows that the anisotropies characterized by $\Delta > 1$ create a gap that introduces a new scale in the correlators. The entropy saturates and entanglement becomes short range. The finite correlation length in the system takes over and all quantum correlations decay exponentially.

V. CRITICAL VERSUS NON-CRITICAL ENTANGLEMENT

We now turn to analyze the results of the calculations described in the previous two sections.

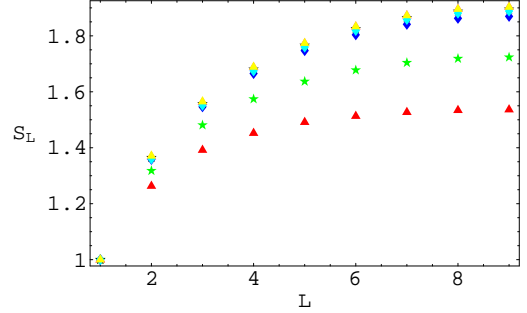


Figure 13: Entropy vs. number of site in rings with different anisotropies. The critical interval is for $\Delta \in (-1, 1]$. The points out of the critical interval are diamonds with $\Delta = 1.5$, stars with $\Delta = 2.0$ and triangles with $\Delta = 2.5$. As we change the anisotropy in the model out of the critical interval, the entropy shows a gap that is greater for increasing values of the anisotropy.

The main picture emerging from these calculations is that there is a clear distinction between the entanglement in a non-critical chain and that in a critical chain, as measured by the entropy S_L of the reduced density matrix ρ_L for L contiguous spins. As exemplified in Figs. (7)-(9), for all non-critical models S_L reaches a saturation value as L increases, whereas for critical chains it grows unboundedly.

A. Non-critical spin chains

Recall that in the non-critical regime, a spin chain is characterized by a gap between the energy of the ground state and that of the first excited state. Relatedly, correlations between increasingly distant spins decay exponentially,

$$\langle \sigma_l^a \sigma_{l+L}^b \rangle - \langle \sigma_l^a \rangle \langle \sigma_{l+L}^b \rangle \sim \exp(-L/\xi), \quad (5.1)$$

where ξ is the correlation length (we take the distance between nearest spins as unit of distance). For non-critical chains, we find that the entropy S_L , a growing function with the block size L , is upper-bounded by a saturation value S^* . This value depends on the parameters specifying the spin chain, and becomes larger as the chain gets closer to a critical point or critical phase. For any fixed value of the parameters specifying the spin model, the saturation value happens to be reached only in the limit of large L , but S_L approaches S^* already for block sizes L of the order of the correlation length ξ . We conclude, therefore, that the entanglement between a block and the rest of an infinite spin chain has a fixed value for blocks larger than the correlation length ξ .

The above calculations can be used not only to obtain S_L , but also to determine the whole spectrum of decreasingly ordered eigenvalues $\{p_L^i\}_{i=1}^{\chi_L}$ of ρ_L (see section VI C). For any L , this spectrum contains only a very small number of relevant eigenvalues, together with many

small eigenvalues with an insignificant overall weight. Thus, in spite of a steady growth of the rank χ_L with L , the effective rank χ_L^{eff} also gets saturated, with the saturation value χ_L^{eff} being essentially reached as S_L reaches S^* .

From a computational point of view, the saturation of ρ_L^{eff} can be used to interpret the extraordinary success of the DMRG in non-critical spin chains and other one-dimensional systems. Only a reduced, upperbounded number of eigenstates of ρ_L must be retained in order to capture the relevant degrees of freedom as L increases [23]. Similarly, a bounded effective rank χ_L^{eff} as a function of L indicates that non-critical spin chains can be efficiently simulated using the techniques introduced in [8].

B. Critical chains

The energy spectrum of a critical spin chain is gapless and the two-spin correlation function is characterized by a power scaling law,

$$\langle \sigma_l^a \sigma_{l+L}^b \rangle - \langle \sigma_l^a \rangle \langle \sigma_{l+L}^b \rangle \sim L^{-q}, \quad (5.2)$$

where $q > 0$ (there are cases where marginal deformations lead to logarithmic corrections to the power law). This scaling law implies an infinite correlation length ξ . For critical spin chains we have obtained that S_L grows unboundedly as a function of L . In particular, in all the cases we have analyzed the growth of S_L is asymptotically given by

$$S_L \sim k \log_2 L, \quad (5.3)$$

where k is either $1/3$ or $1/6$ depending on the parameters of the critical chain. Thus, for critical spin chains the entanglement between a block of spins and the rest of a chain grows unboundedly with the size L of the block, in sharp contrast with the non-critical case. In the next section we will elaborate on the particular shape (5.3) of S_L for critical chains.

Given fixed computer memory and execution time, the DMRG works with significantly smaller accuracy for critical spin chains than for non-critical ones. This result can now be qualitatively interpreted in terms of the arbitrarily large entanglement that links a spin block to the rest of the chain as L grows. Indeed, a larger value of S_L implies that more eigenstates of ρ_L must be retained in order for the DMRG to achieve a similar accuracy as when S_L is small (recall Eq. (2.19)).

Finally, in section VI it will be argued that in 2 (3) dimensions, the entanglement between a block of $L \times L$ (respectively, $L \times L \times L$) spins and the rest of a critical spin lattice grows as L^{D-1} . It can be argued that the same scaling applies to non-critical spin lattices. This implies that χ_L^{eff} grows exponentially with the size of the block, justifying the systematic breakdown of the DMRG in quantum spin systems in more than one dimension.

VI. SCALING OF ENTANGLEMENT AND CFT

The set of results found in the previous sections exemplify the connection between entanglement and quantum field theory concepts. The bridge between quantum information and quantum field theory can be further explored and exploit in both directions. In this sense, we shall translate results from black hole entropy and effective actions on gravitational backgrounds to the language of quantum information. Working in the opposite direction, quantum information natural measures of order based on majorization theory seem to find their way into renormalization group irreversibility. The cross-fertilization of these ideas requires a change of language and quite a lot of background on quantum field theory that we cannot cover here in a self-contained or satisfactory way. Nevertheless, we will very briefly review some concepts in conformal field theory and c-theorem necessary to state their spinoff in quantum information theory.

A. Entropy and conformal field theory

The study of entropy in systems with an infinite number of degrees of freedom has received quite some attention in the context of quantum field theory and black hole physics. Historically, the thermodynamics of a black hole lead to the Bekenstein-Hawking entropy (see for instance [49]). This entropy is associated to the counting of microscopic degrees of freedom inside the horizon and scales as the area of the black hole. Some authors suggested that the origin of this entropy might be rooted in the loss of information forced upon an external observer by the existence of a horizon. Although this point of view is no longer pursued, its analysis comes naturally due to the combination of quantum mechanics and general relativity which underlies the holographic principle. The field theoretical definition of entropy faces the traditional problem of renormalization in quantum field theory and receives the name of fine-grained entropy as well as geometric entropy.

Three computations of genuine quantum field theory entropy are worth recalling. First, Srednicki [18] considered a properly regularized massless bosonic field theory in a universe which is divided by an imaginary sphere of radius R into its inside and outside parts. He then numerically constructed the density matrix of the reduced outside system and found that its entropy scaled with an area law in 3+1 dimensions. For 1+1 dimensions, the scaling behavior of the entropy was found to be logarithmic. Second, Callan and Wilczek [19] put forward the concept of geometric entropy in 1+1 dimensions. There, the power of conformal symmetry was used at full steam in order to compute the entropy of a conformal field theory when reduced to a finite geometry. We shall come back to this result shortly. Finally, the third relevant computation was carried out by Fiola, Preskill, Strominger and Trivedi [20] who mapped a regularized field

theory in 1+1 dimension to the Rindler coordinates and recovered the logarithmic behavior of the microscopic entropy. All these computations needed an explicit ultraviolet regulator since the entropy is an extensive quantity and quantum field theory contains infinitely many degrees of freedom. Note that in our case spin chains come equipped with the intrinsic ultraviolet cutoff of the lattice spacing.

Although more restrictive in scope, the computation of the geometric entropy of a 1+1 dimensional field theory brings the advantage that the result is casted in terms of the parameters that classify conformal field theories. More concretely, the result found by Holzhey, Larsen and Wilczek [21] reads

$$S_L = \frac{c + \bar{c}}{6} \log_2 L \quad (6.1)$$

where c and \bar{c} are the so called central charges for the holomorphic and antiholomorphic sectors of the conformal field theory.

Let us briefly recall that conformal field theories [50] are classified by the representations of the conformal group in 1+1 dimensions. The operators of the theory fall into a structure of highest weight operators and its descendants. Each highest weight operator carries some specific scaling dimensions which dictates those of its descendants. The operators close an algebra implemented into the operator product expansion. One operator is particularly important: the energy-momentum tensor $T_{\mu\nu}$. It is convenient to introduce holomorphic and antiholomorphic indices defined by the combinations $T = T_{zz}$ and $\bar{T} = T_{\bar{z}\bar{z}}$ where $z = x^0 + ix^1$ and $\bar{z} = x^0 - ix^1$. The central charge of a conformal field theory is associated to the coefficient of the correlator

$$\langle 0|T(z)T(0)|0\rangle = \frac{c}{2z^4} \quad (6.2)$$

and the analogous result for \bar{c} in terms of the correlator $\langle 0|\bar{T}(z)\bar{T}(0)|0\rangle$. A conformal field theory is characterized by its central charge, the scaling dimensions h_i and the coefficients of the operator product expansion. Furthermore, unitary theories with $c < 1$ only exist for discrete values of c and are called minimal models. The lowest lying theory corresponds to $c = \frac{1}{2}$ and represents the universality class of a free fermion.

The central charge plays many roles in a conformal field theory. It was introduced above as the coefficient of a correlator of energy-momentum tensors, which means that it is an observable. The central charge also characterizes the response of a theory to a modification of the background metric where it is defined. Specifically, the scale anomaly associated to the lack of scale invariance produced by a non-trivial background metric is

$$\langle 0|T_\mu^\mu|0\rangle = -\frac{c}{12}R \quad (6.3)$$

where R is the curvature of the background metric. This anomaly can also be seen as the emergence of a non-local effective action when the field theory modes are integrated in a curved background.

The results we have found in our analysis match perfectly the geometric entropy computation. In the case of the XX and Heisenberg spin chains the central charge is $c = \bar{c} = 1$ and the model falls into the free boson universality class. The quantum Ising model corresponds to a free fermion, thus $c = \bar{c} = \frac{1}{2}$. The central charge of the theory is seen to play the role of a measure of entanglement. The vacuum of a theory of free bosons is more entangled than the one corresponding to a theory of free fermions. Scaling of entanglement is just another manifestation of the ubiquitous organizing principle orchestrated by conformal symmetry. The amount of surprise obtained when a new degree of freedom is added in a given theory must follow scaling as dictated by the representation of conformal symmetry corresponding to that theory. Because the entropy of the reduced density matrix of the ground state is not attached to any particular operator, it is natural that the central charge is the parameter in control of this measure of entanglement.

Due to the relation between entanglement and the central charge a number of further connections appear. Entanglement does quantify quantum correlations as well as *e.g.* the trace anomaly. The more quantum correlated the vacuum is, the stronger the breaking of conformal symmetry appears when a curved background is present. More relevant is how the theorem on irreversibility of renormalization group flows translates to entanglement in a way that will be discussed shortly.

B. Entanglement in higher dimensional systems

Entanglement in spin chains obeys logarithmic scaling. This result was seen to emerge from conformal symmetry. It is then possible to apply similar arguments in higher dimensions and complete them with standard arguments based on the Schmidt decomposition.

Let's consider a $d+1$ dimensional theory at its critical point. Its ground state is a pure state. Following Srednicki [18], one could now consider the reduced system on *e.g.* a hypersphere S^{d-1} of radius R . The division into the interior A and the exterior B of this imaginary hypersphere can be used to write the ground state using the Schmidt decomposition in terms of pure states $|\xi_i\rangle, |\phi_i\rangle$ associated to each subspace

$$|0\rangle = \sum_i \sqrt{p_i} |\xi_i\rangle_A |\phi_i\rangle_B, \quad (6.4)$$

where p_i are positive numbers and the sum ranges up to the minimum of the dimensions of the Hilbert spaces for A and B . The standard argument follows that both reduced density matrices share the same eigenvalues p_i and, thus, the same entropy. Yet, both systems only share the hypersurface separating them, so that the leading term of the entropy as any infrared cutoff is sent to infinity and the ultraviolet cutoff x_0 is sent to zero must scale as

its “area”

$$S_R = c_1 \left(\frac{R}{x_0} \right)^{d-1} \quad (6.5)$$

where c_1 is a known coefficient related to anomalies that we shall discuss later. This leading scaling law for $x_0 \rightarrow 0$ also holds for massive particles as checked by explicit calculations in free massive theories [52]. The “area” law associated with the hypersurface is understood as an effect coming from the loss of coherence between the points at each side of the boundary separating the interior and exterior parts of the universe. It is then natural to expect that microscopic condensed matter systems will follow the same law.

At variance with spin chains, the ultraviolet cutoff x_0 gets now mixed with the global coefficient c_1 and it is unclear how to extract observable information from the latter. It has been shown that c_1 corresponds to the coefficient of the linear term in the curvature in the effective action of a field theory in a non-trivial gravitational background [52]. Then, c_1 equals $1/6$ for scalar particles and $1/12 \cdot 2^{[d/2]}$ for Dirac fermions. More precisely, every fermionic component contributes to c_1 as half a boson. In $1+1$ dimensions, we worked with spinless fermions, thus the relative factor of 2 between $1/6$ for the Quantum Ising model and $1/3$ for the XY and Heisenberg chains. In dimension $3+1$, the entropy of a system of a free Dirac fermion will carry twice more entropy than a free boson since the Dirac fermion is made of four components.

Entanglement is thus also connected to effective action of quantum field theories on gravitational backgrounds. It is a remarkable fact that in $1+1$ dimensions the effective action has a unique non-local form proportional to the central charge c . When this non-local action is expanded in powers of the curvature, all terms carry the dependence in c . It follows that the trace anomaly, which is a derivative of this effective action with respect to the metric, is also proportional to the central charge. This is no longer true in higher dimensions. The effective action of a quantum field theory defined on a gravitational background develops infinitely many apparently unrelated structures. The entropy of entanglement seems to be related to c_1 [52], the coefficient of the linear term in the curvature R (called a_1 in [53]). On the other hand, other contributions to the trace anomaly giving rise to the Euler density and to non-trivial two-point energy-momentum tensor correlators are related to the structures that come quadratic with the curvature. All the coefficients in the effective action seem to quantify different aspects of entanglement.

A remarkable result concerning the saturation of entanglement in non-critical systems can also be translated from quantum field theory to spin chains. It has been proven that the leading order result when the ultraviolet cutoff is sent to infinity that we have quoted above is not modified by adding a mass to the scalar field. The leading behavior of entanglement is not affected by going away from conformal symmetry because the contribution

to the entropy comes from the entanglement loss of points near each side of the boundary (see also [51]). The scaling law in terms of the hypersurface separating them is respected although a finite correlation length is present. Moreover, the subleading corrections to the “area” law are known when $x_0 \ll \frac{1}{m} \ll L$, L being an infrared cut-off which defines a separation of space in two regions in analogy to our previous R ,

$$S_m - S_{m=0} = \begin{cases} -\frac{Lm}{24\pi} & d = 2 + 1 \\ \frac{L^2 m^2}{96\pi^2} \ln mx_0 & d = 3 + 1 \end{cases} \quad (6.6)$$

where the subindex m labels the massive theory. The case $d = 1 + 1$ corresponds to the universality class we have been discussing in systems of spin chains and yields the following result [52]

$$S = -\frac{1}{6} \ln mx_0 \quad x_0 \ll \frac{1}{m} \ll L . \quad (6.7)$$

This latter result is indeed observed in our computation.

The lack of saturation of entanglement in massive theories have clear implications for the application of DMRG techniques as well as other modifications of the Wilsonian block-spin idea for condensed matter systems. Entanglement always diverges (even off criticality) in more than $1+1$ dimensions and limits the success of such an approach. It seems conceptually preferable to construct projections of the exact renormalization group based in momentum space as the local potential approximation. This method has proven quite powerful in scalar theories [54] where it provides good approximations to critical exponents in any number of dimensions and can even detect triviality.

C. Majorization and entanglement

Let us return to quantum spin chains where entanglement pervades the system at conformal points. The absence of a mass scale makes the quantum correlations to extend to long distances. Consequently, the vacuum structure must describe this fact and the entropy shows scaling as discussed above. It is arguable that the entropy of the vacuum in the reduced system is just one out of many possible measures of entanglement. Then, other yet unexplored measures of entanglement may bring further information about the structure of the vacuum.

In order to investigate this issue, we can further exploit our computations due to the fact that we have explicit results for the density matrix of the vacuum in the XX model without magnetic field. The 2^L eigenvalues of ρ_L correspond to the product of those coming from the correlators,

$$\lambda_{x_1 x_2 \dots x_L} = \prod_{m=0}^{L-1} \frac{1 + (-1)^{x_m} \nu_m}{2}, \quad x_m = 0, 1 \ \forall m. \quad (6.8)$$

It is convenient to first visualize the typical shape of eigenvalues $(1 \pm \nu_m)/2$ and observe that they are concentrated on the values 0 and 1. Each mode tends to remember its pure state origin. Furthermore, most of the ρ_L eigenvalues are almost zero or one, due to the product structure in Eq.(6.8) and only a small set will take intermediate values, bringing the main contribution to the entropy.

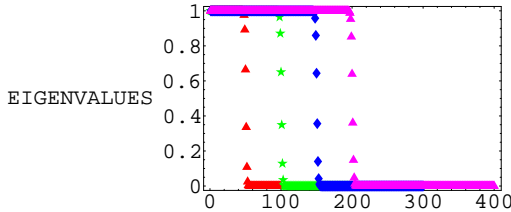


Figure 14: Plot of all the eigenvalues $\frac{1 \pm \nu_m}{2}$ for the Ising model and $L = \{50 \text{ (triangles)}, 100 \text{ (stars)}, 150 \text{ (diamonds)}, 200 \text{ (triangles)}\}$. As L increases new modes are populated.

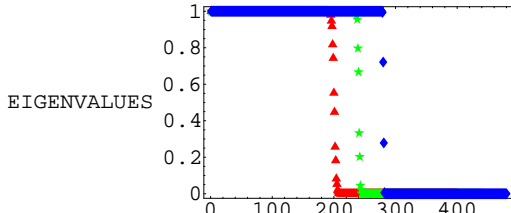


Figure 15: Plot of the eigenvalues $\frac{1 \pm \nu_m}{2}$ for the XX model as a function of λ taking $L = 200$ spins from an infinite ring. Triangles display the eigenvalues for $\lambda = 0.5$, stars for $\lambda = 0.999$ and diamonds the eigenvalues for $\lambda = 0.99999$. When λ approaches 1, the ground state becomes a product state and the modes take only the value one or zero. Initially, the three plots overlap each other. The figure is displayed in such a way that every plot is shifted 40 points respect to the previous one.

The eigenvalues of ρ_L form a probability distribution. It is easy to numerically verify that at conformal points

$$\rho_{L+2} \prec \rho_L, \quad (6.9)$$

that is, the probability distributions associated to the density matrices obey a majorization relation. Due to the spin structure of the problem the majorization takes

place at two-spin steps. We have verified that a similar result holds for the quantum ising model at its critical point.

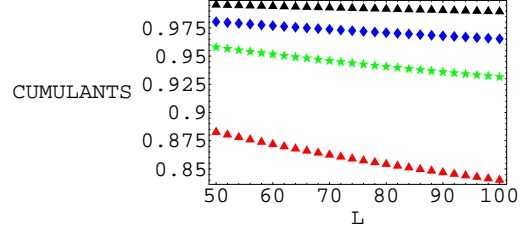


Figure 16: Plot of the cumulants of the eight (triangles), sixteen (stars), thirty two (diamonds) and sixty four (triangles) larger probabilities associated to the ground state ρ_L as a function of L in steps of 2 in the XX model without magnetic field.

The increase of amount of surprise quantified by the entropy is rooted in a deeper sense of ordering in the vacuum. The ground state becomes more and more disordered as dictated by a majorization arrow. Note that this implies an increasing number of relations between the eigenvalues of ρ_L as L goes to infinity. The vacuum in a field theory is far more ordered than what the scaling of entropy hints at.

In order to establish the role of majorization and its relation to conformal symmetry, further work is necessary. In particular, marginal deformations need to be analyzed carefully. Later on we shall argue that a different type of majorization seems to hold along renormalization group flows. In that case, L is kept fixed but the parameters of the hamiltonian change as dictated by renormalization group transformations.

D. Irreversibility of entanglement and the c-theorem

Given the relation between entanglement and conformal symmetry, some powerful quantum field theory results can be borrowed and translated to quantum information parlance. It is of particular relevance the so called Zamolodchikov's c-theorem [24] that establishes that the central charge of a unitary 1+1 dimensional theory always decreases along renormalization group trajectories. The existence of a c-theorem in more than two dimensions has been a subject of a lot of effort [55, 56, 57, 58, 59] and a proof has been proposed in [60]. Zamolodchikov's theorem in two dimensions can be proven using the spectral densities following Ref. [56]. Consider the spectral representation of the correlator for two energy-momentum tensors (the energy-momentum

operator is defined for any quantum field theory and corresponds to a descendant of the identity)

$$\begin{aligned} \langle 0 | T_{\alpha\beta}(x) T_{\mu\nu}(0) | 0 \rangle &= \\ &= \frac{\pi}{3} \int d\lambda c(\lambda, \mu) (p_\alpha p_\beta - p^2 g_{\alpha\beta}) (p_\mu p_\nu - p^2 g_{\mu\nu}) G(x, \lambda) \end{aligned} \quad (6.10)$$

where λ is the spectral parameter (with dimensions of mass), $c(\lambda, \mu)$ is the spectral function, which depends on λ and on the subtraction point μ , and $G(x, \lambda)$ is the free scalar propagator of a particle with mass λ . At a fixed point, the spectral function reduces to a delta function $c(\lambda, \mu)|_{cft} = c \delta(\lambda)$, where the coefficient c is a constant, reflecting the fact that all physical intermediate states are massless. The UV fixed point can be analyzed taking $x \rightarrow 0$ and it follows that

$$c_{UV} = \int d\lambda c(\lambda, \mu). \quad (6.11)$$

where c_{UV} is the central charge of the ultraviolet theory. On the other hand, in the IR limit only massless modes survive, so that the spectral function can in general be written as

$$c(\lambda, \mu) = c_{IR} \delta(\lambda) + c_{\text{smooth}}(\lambda, \mu), \quad (6.12)$$

where the contribution of all massive modes is contained in $c_{\text{smooth}}(\lambda, \mu)$. It thus follows that

$$c_{UV} = c_{IR} + \int d\lambda c_{\text{smooth}}(\lambda, \mu), \quad (6.13)$$

where the second term on the r.h.s. is necessarily μ -independent. Finally, unitarity guarantees that c_{smooth} is positive, so

$$c_{UV} \geq c_{IR}. \quad (6.14)$$

This result can be understood as a net decrease of degrees of freedom as weighted by the central charge along renormalization group trajectories. Note also these ideas match bosonization: in two dimensions two Majorana fermions can be made into a boson. All proposed generalizations of the central charge in more than two dimensions are based on the trace anomaly and share the property that fermions weight more than bosons. Exact bosonization is then not possible. Moreover, long distance realizations should tend to favor bosons in uncanny cooperation with the Goldstone theorem [61].

The c-theorem immediately implies that entanglement decreases along renormalization group flows, that is, the entropy of the reduced density matrix decreases along renormalization group trajectories,

$$S_L^{UV} > S_L^{IR}. \quad (6.15)$$

The decoupling of the massive modes in the spectrum at long distances irreversibly reduces the amount of non-local quantum correlations in the system. This result is

only valid for unitary theories and is not obvious because a renormalization group transformation in quantum field theory is made of two steps: integration of high-energy modes followed by rescaling. While the first step seems to imply irreversibility, the second makes it obscure. Furthermore, the proper construction of this result implies a careful treatment of renormalization. The role of unitarity is dominant since counterexamples can be built where renormalization group flows form limit cycles for non-unitary theories. Entanglement loss and unitarity are, thus, related.

There is an explicit result we have already presented that can be used to illustrate the loss of entanglement along renormalization group trajectories. Consider the non-critical massive boson. The departure from the massless case corresponds to adding a relevant operator. The flow will make the mass grow. The renormalization group trajectory is driven by the increase of the mass. It must follow from the two-dimensional c-theorem that for increasing mass, the entropy of the system decreases. This is indeed the case as verified in Eq. 6.7

$$S_{L,m_1} - S_{L,m_2} = -\frac{1}{6} \ln \frac{m_1}{m_2} < 0 \quad m_1 > m_2. \quad (6.16)$$

A perturbative c-theorem is also known to hold in any dimension and, again, it can be checked on Eq. 6.6

$$S_{L,m} - S_{L,m=0} < 0. \quad (6.17)$$

Furthermore the decrease of the entropy is monotonous in m .

It is natural to try to go one step further and try to relate irreversibility of the renormalization group to the majorization properties that may structure the entanglement in the vacuum. Our preliminary numerical results seem to indicate that

$$\rho_L^{m=0} \prec \rho_L^m \quad (6.18)$$

in spin chains, in all the analytical results shown in Eqs.(6.6, 6.7) and in the computation produced by Srednicki [18]. Although all the above cases correspond to renormalization group flows driven by a simple massive deformation, one then may speculate that

$$\rho_L^{UV} \prec \rho_L^{IR} \quad (6.19)$$

and that majorization is indeed underlying the irreversibility of renormalization group flows. This, though, remains a conjecture.

Acknowledgments

We acknowledge fruitful discussions with R. Emparan and A. Kitaev. This work was supported by the by the Spanish grants GC2001SGR-00065 and MCYT FPA2001-3598, by the National Science Foundation of USA under grant EIA-0086038, and by the European Union under grant ISF1999-11053.

Appendix A: SPECTRUM OF H_{XY}

In this appendix we determine the ground state $|\Psi_g\rangle$ of the XY model with open boundary conditions,

$$H_{XY} = - \sum_{l=-\frac{N}{2}+1}^{\frac{N}{2}-1} \left(\frac{1+\gamma}{2} \sigma_l^x \sigma_{l+1}^x + \frac{1-\gamma}{2} \sigma_l^y \sigma_{l+1}^y \right) - \sum_{l=-\frac{N}{2}+1}^{\frac{N}{2}} \lambda \sigma_l^z, \quad (\text{A1})$$

in the limiting case of an infinite chain, $N \rightarrow \infty$.

a. Jordan-Wigner Transformation

The initial spin operators satisfy anticommutation rules at any given site but follow commutation rules at separate sites. The non-local Jordan-Wigner transformation maps these operators into fully anticommuting spinless fermions defined by

$$\hat{a}_l = \left(\prod_{m < l} \sigma_m^z \right) \frac{\sigma_l^x + i\sigma_l^y}{2} \quad (\text{A2})$$

$$\{\hat{a}_l^\dagger, \hat{a}_m\} = \delta_{lm}, \quad \{\hat{a}_l, \hat{a}_m\} = 0.$$

In terms of operators \hat{a} the above Hamiltonian becomes

$$H_{XY} = \frac{1}{2} \sum_{l=-\frac{N}{2}+1}^{\frac{N}{2}-1} [(\hat{a}_{l+1}^\dagger \hat{a}_l + \hat{a}_l^\dagger \hat{a}_{l+1}) + \gamma (\hat{a}_l^\dagger \hat{a}_{l+1}^\dagger + \hat{a}_{l+1} \hat{a}_l)] - \lambda \sum_{l=-\frac{N}{2}+1}^{\frac{N}{2}} \hat{a}_l^\dagger \hat{a}_l. \quad (\text{A3})$$

b. Fourier Transformation

We can now exploit the (quasi) translational symmetry of the system by introducing Fourier transformed fermionic operators

$$\hat{d}_k = \frac{1}{\sqrt{N}} \sum_{l=-\frac{N}{2}+1}^{\frac{N}{2}-1} \hat{a}_l e^{-i\frac{2\pi}{N}kl}, \quad (\text{A4})$$

$-N/2+1 \leq k \leq N/2$. Due to the fact that this transformation is unitary, the anticommutation relations remain valid

$$\{\hat{d}_k^\dagger, \hat{d}_p\} = \delta_{kp} \quad \forall\{k, p\}. \quad (\text{A5})$$

The Hamiltonian now takes an almost diagonal form,

$$H = \sum_{k=-N/2+1}^{N/2} (-\lambda + \cos \frac{2\pi k}{N}) \hat{d}_k^\dagger \hat{d}_k + \frac{i\gamma}{2} \sum_{k=-N/2+1}^{N/2} \sin \frac{2\pi k}{N} (\hat{d}_k \hat{d}_{-k} + \hat{d}_k^\dagger \hat{d}_{-k}^\dagger). \quad (\text{A6})$$

where an extra term, suppressed by $\frac{1}{N}$, should be present. We shall though ignore it here since our results concern the limit $N \rightarrow \infty$.

c. Bogoliubov Transformation

A final unitary transformation is needed to cast the Hamiltonian into a manifestly free particle theory. This so-called Bogoliubov transformation can be expressed as

$$\begin{aligned} \hat{b}_k^\dagger &= u_k \hat{d}_k^\dagger + i v_k \hat{d}_{-k} \\ \hat{b}_k &= u_k \hat{d}_k - i v_k \hat{d}_{-k}^\dagger, \end{aligned} \quad (\text{A7})$$

where $u_k = \cos \theta_k / 2$, $v_k = \sin \theta_k / 2$ for

$$\cos \theta_k = \frac{-\lambda + \cos \frac{2\pi k}{N}}{\sqrt{(\lambda - \cos \frac{2\pi k}{N})^2 + \gamma^2 \sin^2 \frac{2\pi k}{N}}}. \quad (\text{A8})$$

Again, due to unitarity of the Bogoliubov transformation the operators $\{\hat{b}_k\}$ follow the usual anticommutation relation

$$\{\hat{b}_k^\dagger, \hat{b}_p\} = \delta_{kp} \quad \forall\{k, p\}. \quad (\text{A9})$$

Finally, the Hamiltonian takes a diagonal form

$$H = \sum_{k=-N/2+1}^{N/2} \tilde{\Lambda}_k \hat{b}_k^\dagger \hat{b}_k, \quad (\text{A10})$$

where

$$\tilde{\Lambda}_k \equiv \sqrt{\left(\lambda - \cos \frac{2\pi k}{N} \right)^2 + \gamma^2 \sin^2 \frac{2\pi k}{N}}. \quad (\text{A11})$$

The thermodynamical limit is obtained by defining $\phi = 2\pi k/N$ and taking the $N \rightarrow \infty$ limit

$$H = \int_{-\pi}^{\pi} \frac{d\phi}{2\pi} \Lambda_\phi \hat{b}_\phi^\dagger \hat{b}_\phi, \quad (\text{A12})$$

with

$$\Lambda_\phi^2 = (\lambda - \cos \phi)^2 + \gamma^2 \sin^2 \phi. \quad (\text{A13})$$

Appendix B: CORRELATION MATRIX FOR THE XY MODEL

In this section we show how to obtain the correlation matrix $\langle \check{a}_m \check{a}_n \rangle$ of the ground state of the Hamiltonian

$$\begin{aligned} H_{XY} = & i \sum_{l=-\frac{N}{2}+1}^{\frac{N}{2}-1} \left(\frac{1+\gamma}{2} \check{a}_{2l} \check{a}_{2l+1} - \frac{1-\gamma}{2} \check{a}_{2l-1} \check{a}_{2l+2} \right) \\ & + i \sum_{l=-\frac{N}{2}+1}^{\frac{N}{2}} \lambda \check{a}_{2l-1} \check{a}_{2l}, \end{aligned} \quad (\text{B1})$$

where the Majorana operators \check{a} fulfill

$$\check{a}_m^\dagger = \check{a}_m, \quad \{a_m, a_n\} = 2\delta_{mn}, \quad (\text{B2})$$

$$-N+1 \leq m, n \leq N.$$

We start by diagonalizing the above Hamiltonian. This can be achieved by means of two canonical transformations. Let us define $2N$ auxiliary Majorana operators \check{d} and \check{e} ,

$$\begin{bmatrix} \check{d}_{2k-1} \\ \check{d}_{2k} \end{bmatrix} = \sqrt{\frac{2}{N}} \sum_{l=-\frac{N}{2}+1}^{\frac{N}{2}} \cos \frac{2\pi kl}{N} \begin{bmatrix} \check{a}_{2l-1} \\ \check{a}_{2l} \end{bmatrix}, \quad (\text{B3})$$

$$\begin{bmatrix} \check{e}_{2k-1} \\ \check{e}_{2k} \end{bmatrix} = \sqrt{\frac{2}{N}} \sum_{l=-\frac{N}{2}+1}^{\frac{N}{2}} \sin \frac{2\pi kl}{N} \begin{bmatrix} \check{a}_{2l-1} \\ \check{a}_{2l} \end{bmatrix}, \quad (\text{B4})$$

$0 \leq k \leq N/2$, that take the Hamiltonian into sum of Hamiltonians H_k ,

$$H_{XY} = \sum_{k=0}^{N/2} H_k, \quad (\text{B5})$$

where

$$H_k = \frac{i\tilde{\Lambda}_k}{4} \begin{bmatrix} d_{2k-1} \\ e_{2k-1} \\ d_{2k} \\ e_{2k} \end{bmatrix}^T \begin{bmatrix} 0 & 0 & c_k & -s_k \\ 0 & 0 & s_k & c_k \\ -c_k & -s_k & 0 & 0 \\ s_k & -c_k & 0 & 0 \end{bmatrix} \begin{bmatrix} d_{2k-1} \\ e_{2k-1} \\ d_{2k} \\ e_{2k} \end{bmatrix}, \quad (\text{B6})$$

$c_k \equiv \cos \theta_k$, $s_k \equiv \sin \theta_k$. The diagonalization is completed by a second transformation that acts independently for each value of k , according to

$$\begin{bmatrix} b_{-2k-1} \\ b_{-2k} \\ b_{2k-1} \\ b_{2k} \end{bmatrix} = \frac{1}{\sqrt{2}} \begin{bmatrix} u_k & v_k & u_k & -v_k \\ u_k & v_k & -u_k & v_k \\ v_k & -u_k & v_k & u_k \\ -v_k & u_k & v_k & u_k \end{bmatrix} \begin{bmatrix} d_{2k-1} \\ e_{2k-1} \\ d_{2k} \\ e_{2k} \end{bmatrix}. \quad (\text{B7})$$

In terms of the $2N$ Majorana operators \check{b}_p , $-N+1 \leq p \leq N$, the Hamiltonian is finally written as

$$H_{XY} = \frac{i}{4} \sum_{k=-\frac{N}{2}+1}^{\frac{N}{2}} \tilde{\Lambda}_k (\check{b}_{2k-1} \check{b}_{2k} - \check{b}_{2k} \check{b}_{2k-1}), \quad (\text{B8})$$

as we wanted to show.

The above two orthogonal transformations define $W \in SO(2N)$, where

$$\check{b}_p = \sum_{m=-N+1}^N W_{pm} \check{a}_m, \quad -N+1 \leq p \leq N. \quad (\text{B9})$$

Then, coefficients g_l in Eq. (3.46) are obtained through

$$\Gamma^A = W^T \Gamma^D W, \quad (\text{B10})$$

where

$$\Gamma^B = \bigoplus_{k=-\frac{N}{2}+1}^{\frac{N}{2}} \begin{bmatrix} 0 & 1 \\ -1 & 0 \end{bmatrix}. \quad (\text{B11})$$

Appendix C: ANALYTICAL EVALUATION OF THE CORRELATION MATRIX FOR THE XY MODEL

In this appendix we present an analytical expression for g_l , Eq. (3.47), for five particular cases of the XY chain.

d. Ferromagnetic limit

The ferromagnetic limit corresponds to $\lambda \rightarrow \infty$. In this case, it is easy to see that

$$g_l = \delta_{l0} \quad \forall \gamma. \quad (\text{C1})$$

e. Ising model

For an Ising model, $\gamma = 1$, with magnetic field λ we have

$$g_l = \frac{1}{2\pi} \int_{-\pi}^{\pi} d\phi e^{-il\phi} \frac{e^{-i\phi} - \lambda}{\sqrt{1 - \lambda e^{i\phi}} \sqrt{1 - \lambda e^{-i\phi}}}. \quad (\text{C2})$$

For values of $\lambda \in [-1, +1]$,

$$(1 - \lambda e^{i\phi})^{-\frac{1}{2}} = \sum_{m=0}^{\infty} \frac{(2m-1)!!}{(2m)!!} \lambda^m e^{i\phi m}, \quad (\text{C3})$$

where

$$(2m)!! = 2^m m! \quad (2m-1)!! = \frac{(2m)!}{2^m m!}, \quad (\text{C4})$$

obtaining the equation

$$g_l =$$

$$\begin{cases} \sum_{m=0}^{\infty} \left(\frac{(2(m+l+1))!}{(2^{m+l+1}(m+l+1)!)^2} - \frac{(2(m+l))!}{(2^{m+l}(m+l)!)^2} \right) \\ \frac{(2m-1)!!}{(2m)!!} \lambda^{2m+l+1} & l \geq 0, \\ \left(\sum_{m=-l-1}^{\infty} \frac{(2(m+l+1))!}{(2^{m+l+1}(m+l+1)!)^2} - \sum_{m=-l}^{\infty} \frac{(2(m+l))!}{(2^{m+l}(m+l)!)^2} \right) \\ \frac{(2m-1)!!}{(2m)!!} \lambda^{2m+l+1} & l \leq 0. \end{cases} \quad (\text{C5})$$

For the limits $\lambda = 0$ or $\lambda = 1$ these equations reduce to

a. *Ising model without magnetic field*.- The Ising model is recovered for $\gamma = 1$. When no magnetic field is present, $\lambda = 0$ and g_l reduces to

$$g_l = \delta_{-l1}. \quad (\text{C6})$$

b. *Ising model in a critical magnetic field*.- For the Ising model, $\gamma = 1$, and when the magnetic field is in the critical point $\lambda = 1$, the initial expression for g_l transforms to,

$$\begin{aligned} g_l &= \int_0^\pi \frac{d\phi}{\pi} \frac{(-1 + \cos \phi) \cos \phi l - \sin \phi \sin \phi l}{\sqrt{(1 - \cos \phi)^2 + \sin^2 \phi}} \\ &= \int_0^\pi -\frac{d\phi}{\pi} \sin \left(l + \frac{1}{2} \right) \phi = \frac{-1}{\pi (l + \frac{1}{2})}. \end{aligned} \quad (\text{C7})$$

f. XX model with magnetic field

The XX model corresponds to $\gamma = 0$ with a magnetic field in the range given by $\lambda \in [-1, 1]$. Making a small transformation in the general expression, we get

$$\begin{aligned} g_l &= \int_0^\pi \frac{d\phi}{\pi} \frac{-\lambda + \cos \phi}{|\lambda - \cos \phi|} \cos l\phi \\ &= \frac{1}{\pi} \left(\int_0^{\phi_c} \cos l\phi d\phi - \int_{\phi_c}^\pi \cos l\phi d\phi \right) \\ &= \frac{2}{l\pi} \sin l\phi_c, \quad \phi_c = \arccos(\lambda). \end{aligned} \quad (\text{C8})$$

In the particular subcase of the XX model without magnetic field, $\lambda = 0$, we obtain

$$g_l = \frac{2}{l\pi} \sin \frac{l\pi}{2}, \quad (\text{C9})$$

which is equivalent to

$$\begin{aligned} g_l &= 0, \quad l \in \text{even} \\ g_l &= \frac{2}{l\pi} (-1)^{(l-1)/2}, \quad l \in \text{odd}. \end{aligned} \quad (\text{C10})$$

g. The XY model with critical magnetic field

For any anisotropy $|\gamma| \leq 1$ and critical magnetic field, $\lambda = 1$, the general expression is recast into,

$$\begin{aligned} g_l &= \int_0^\pi \frac{d\phi}{\pi} \frac{(\cos \phi - 1) \cos l\phi - \gamma \sin \phi \sin l\phi}{\sqrt{(1 - \cos \phi)^2 + \gamma^2 \sin^2 \phi}} \\ &= -\frac{\gamma + 1}{2\pi} \int_0^\pi d\phi \frac{\sin(l + \frac{1}{2})\phi}{\sqrt{\sin^2 \phi/2 + \gamma^2 \cos^2 \phi/2}} \\ &\quad - \frac{\gamma - 1}{2\pi} \int_0^\pi d\phi \frac{\sin(l - \frac{1}{2})\phi}{\sqrt{\sin^2 \phi/2 + \gamma^2 \cos^2 \phi/2}} \end{aligned} \quad (\text{C11})$$

h. The XY model without magnetic field

Finally, following reference [62] the limit of the XY model without magnetic field corresponds to g_l expressed as follows:

$$\begin{aligned} g_l &= - \left(\frac{1 + \gamma}{2} L_{l+1} + \frac{1 - \gamma}{2} L_{l-1} \right) \quad l \in \text{odd} \\ g_l &= 0 \quad l \in \text{even}, \end{aligned} \quad (\text{C12})$$

where,

$$L_l = \frac{2}{\pi} \int_0^{\pi/2} d\phi \frac{\cos \phi l}{\sqrt{\cos^2 \phi + \gamma^2 \sin^2 \phi}}. \quad (\text{C13})$$

A series expansion of this integral is given by:

$$\begin{aligned} L_l(\gamma) &= (-1)^{l/2} \frac{2}{1 + \gamma} \\ &\quad \left(h_0 h_{l/2} - \frac{\ln 1 - \alpha^2}{\pi} - \sum_{r=1}^{\infty} \alpha^{2r} \left(\frac{1}{r\pi} - h_r h_{r+(l/2)} \right) \right) \end{aligned} \quad (\text{C14})$$

where,

$$h_l = 2^{2l} \binom{2l}{l} \quad \alpha = \frac{1 - \gamma}{1 + \gamma}. \quad (\text{C15})$$

[1] C. H. Bennett and D. P. DiVincenzo, *Nature* **404**, 247 (2000).

[2] M. A. Nielsen and I. L. Chuang, "Quantum computation and quantum information" Cambridge Univ. Press.

[3] Special issue on experimental proposals for quantum computation, *Fortschr. Phys.* **48**, No. 9–11 (2000).

[4] J. Preskill, *J. Mod. Opt.* **47**, 127 (2000), *quant-ph/9904022*.

[5] J. Bardeen, L. N. Cooper and J. R. Schrieffer, *Phys. Rev.* **108**, 1175 (1957).

[6] R. B. Laughlin, *Phys. Rev. Lett.* **50**, 1395 (1983).

[7] S. Sachdev, *Quantum Phase Transitions* (Cambridge Univ. Press, 1999).

[8] G. Vidal, *in preparation*.

[9] G. Vidal, J. I. Latorre, E. Rico and A. Kitaev, to appear in *Phys. Rev. Lett.*, *quant-ph/0211074*.

[10] V. Coffman, J. Kundu, W. K. Wootters, *Phys. Rev. A* **61** 052306 (2000), *quant-ph/9907047*.

[11] K. M. O'Connor and W. K. Wootters, *Phys. Rev. A* **63**, 052302 (2001), *quant-ph/0009041*.

[12] M. C. Arnesen, S. Bose and V. Vedral, *quant-ph/0009060* (2001)

[13] D. Gunlycke, S. Bose, V.M. Kendon, V. Vedral, *Phys. Rev. A* **64**, 042302 (2001), *quant-ph/0102137*.

[14] P. Zanardi and X. Wang, *J. Phys. A* **35**, 7947 (2002), *quant-ph/0201028*.

[15] T. J. Osborne and M. A. Nielsen, *quant-ph/0202162*.

[16] A. Osterloh, L. Amico, G. Falci and R. Fazio, *Nature* **416**, 608 (2002), *quant-ph/0202029*.

[17] M. A. Martín-Delgado, *quant-ph/0207026*.

[18] M. Srednicki, *Phys. Rev. Lett.* **71**, 666 (1993), *hep-th/9303048*.

[19] C. G. Callan and F. Wilczek, *Phys. Lett.B* **333** (1994) 55, *hep-th/9401072*.

[20] T. M. Fiola, J. Preskill, A. Strominger and S. P. Trivedi, *Phys. Rev. D* **50** (1994) 3987, *hep-th/9403137*.

[21] C. Holzhey, F. Larsen and F. Wilczek, *Nucl.Phys.B* **424** (1994) 443, *hep-th/9403108*.

[22] S. R. White, *Phys. Rev. B* **48**, 10345 (1993).

[23] S. Rommer and S. Östlund, "Density matrix renormalization", Dresden, 1998 (Springer, Berlin, 1999), pp 67-89.

[24] A. B. Zamolodchikov, *JETP Lett.* **43** (1986) 730.

[25] For an overview and references see *Quan. Inf. Comp.* **1** (2001) .

[26] C. H. Bennett, H. J. Bernstein, S. Popescu and B. Schumacher, *Phys. Rev. A* **53**, 2046 (1996), *quant-ph/9511030*.

[27] G. Vidal, *J. Mod. Opt.* **47**, 355 (2000), *quant-ph/9807077*.

[28] M. A. Nielsen, *Phys. Rev. Lett.* **83**, 436 (1999), *quant-ph/9811053*.

[29] A. Acín, G. Vidal, J. I. Cirac, *Quant. Inf. Comp.* **3**, 55 (2003), *quant-ph/0202056*.

[30] F. M. Spedalieri, *quant-ph/0110179*.

[31] W. Dür, G. Vidal, J. I. Cirac, *Phys. Rev. A* **62**, 062314 (2000), *quant-ph/0005115*.

[32] F. Verstraete, J. Dehaene, B. De Moor, H. Verschelde , *Phys. Rev. A* **65** 052112 (2002), *quant-ph/0109033*.

[33] G. Vidal, *quant-ph/0301063*.

[34] W. K. Wootters, *Phys. Rev. Lett.* **80**, 2245 (1998), *quant-ph/9709029*.

[35] E. H. Lieb and M. B. Ruskai, *J. Math. Phys.*, **14** 1938 (1973)

[36] P. Stelmachovic and V. Buzek, presented at a quantum information conference in Gdansk (July 2001) and in San Feliu (March 2002).

[37] R. Bhatia, "Matrix Analysis", Graduate Texts in Mathematics vol. 169, Springer-Verlag, 1996.

[38] M. A. Nielsen and G. Vidal, *Quant. Inf. and Comp.* **1**, 76 (2001).

[39] T. J. Osborne and M. A. Nielsen, *quant-ph/0109024* (2001)

[40] M. C. Chung and I. Peschel *Phys. Rev. B* **64** 064412 (2001), *cond-mat/0103301*.

[41] A. Kitaev, *cond-mat/0010440*.

[42] P. Christe and M. Henkel, "Introduction to conformal invariance and its applications to critical phenomena" Ed. Springer-Verlag m.16.

[43] B. K. Chakrabarti, A. Dutta and P. Sen, "Quantum Ising phases and Transitions in Transverse Ising Models" Ed. Springer m.41

[44] H. Bethe, *Z. Phys.* **71**, 205 (1931).

[45] R. Orbach, *Phys.Rev.* **112**, 309 (1958).

[46] C. N. Yang and C. P. Yang, *Phys.Rev.* **150**, 321 (1966).

[47] J. C. Bonner and M. E. Fisher, *Phys.Rev.* **135**, A640 (1964).

[48] I. Affleck., *J.Phys.A* **31**, 4573 (1998), *cond-mat/9802045*.

[49] J. D. Bekenstein *gr-qc/9409015*.

[50] Paul Ginsparg, "Applied conformal field theory" Les Houches Summer School 1988, pp 1-168.

[51] J. Gaite *Mod. Phys. Lett.* **A16**, 1109 (2001), *cond-mat/0106049*.

[52] D. Kabat and M. J. Strassler *Phys. Lett. B* **329**, 46 (1994) *hep-th/9401125*; D. Kabat *Nucl. Phys. B* **453**, 281 (1995) *hep-th/9503016*.

[53] "Quantum fields in curved space", N. D. Birrell and P. C. W. Davies, Cambridge University Press (1982).

[54] T. R. Morris *Phys. Lett.* **B329**, 241 (1994), *hep-th/9403340*; J. Berges, N. Tetradis and C. Wetterich, *Phys. Rept.* 363, 223 (2002), *hep-ph/0005122*; R. D. Ball et al. *Phys. Lett.* **B347**, 80 (1995), *hep-th/9411122*.

[55] J. L. Cardy, *Phys. Lett.B* **215**, 749 (1988).

[56] A. Cappelli, D. Friedan and J.I. Latorre, *Nucl. Phys. B* **352** (1991) 616.

[57] A. Cappelli, J. I. Latorre and X. Vilasís-Cardona, *Nucl. Phys. B* **376**, 510 (1992), *hep-th/9109041*.

[58] H. Osborn and G.M. Shore, *Nucl. Phys. B* **571**, 287 (2000), *hep-th/9909043*.

[59] D. Anselmi, *Nucl. Phys. B* **567**, 331 (2000), *hep-th/9905005*.

[60] S. Forte and J. I. Latorre, *Nucl. Phys. B* **535** (1998) 709, *hep-th/9805015*.

[61] S. Forte and J. I. Latorre, *hep-th/9811121*.

[62] E. Lieb, T. Schultz and D. Mattis, *Annals of Phys.* **16** 407 (1961).